KWARA STATE UNIVERSITY

COLLEGE OF ENGINEERING AND TECHNOLOGY

DEPARTMENT OF AERONAUTICAL AND ASTRONAUTICAL ENGINEERING

DESIGN AND PERFORMANCE ANALYSIS OF A CENTRIFUGAL COMPRESSOR USED IN MICRO GAS TURBINE FOR UAVs

BY

HABEEB BABATUNDE IDRIS
13/57PH/130

A MAJOR QUALIFYING PROJECT REPORT
IN PARTIAL FULFILLMENT OF THE REQUIREMENTS
FOR THE DEGREE IN BACHELOR OF ENGINEERING
IN AERONAUTICAL AND ASTRONAUTICAL ENGINEERING

MAY 2018

DECLARATION

By submitting this thesis, titled the Design and Performance Analysis of a Centrifugal Compressor Used in Micro Gas Turbines for UAVs by Habeeb Babatunde Idris, I declare that the entirety of this work is solely mine as necessary references have been made to the journals consulted both within the text and in References section. I also declare that this thesis has not been submitted, in entirety or in part, for obtaining any qualification before. It is submitted to the Department of Aeronautical and Astronautical Engineering of Kwara State University, in partial fulfillment of the requirements to obtain a Degree in Bachelor of Engineering.

Supervisor: ……. …….....

Mr Adebayo Mayowa Date

Project Coordinator: …….. ……..

Engr. Sylvester Akiishi Date

Head of Department: ……. ……..

Prof. Suleiman Talabi Date

ACKNOWLEDGEMENT

All glories and adorations are to God Almighty, the lord of the universe, for his infinite mercy and bountiful provisions.

I would not have been able to complete this work if not for certain individuals. I give gratitude to all of them.

To my parents, Alhaji and Alhaja Idris, for providing me with moral, financial, and spiritual supports.

To my supervisor, with his immense knowledge and technical know-how in this field of turbo machinery, for his relentless and unreserved contribution and dedication for the success of this work. To the project coordinator for granting early approval of this project topic.

To Mr Ronald Ajiboye for always giving necessary motivation, advice, guidelines and lots more.

To Engr. Olalekan Olayemi for his usual advice and concerns for the progress and ultimately, the success of this work. To all Aeronautical and Astronautical Engineering staff for their contributions directly and indirectly.

I appreciate my siblings, in persons of Idris Toyeeb, Idris Idris, Idris Abdulmujeeb, and Idris Mujeebat, for their prayers and contributions.

I give my unreserved gratitude to Ambali Hameeda and Afodun Shukurat for their relentless efforts to ensure progressive work on this project and for the warm comfort provided always from the inception of the work till completion.

This acknowledgement will not be complete without the recognition of my colleagues, in persons of Adebayo Abdulganiy, Sambo Hamdallah, Adio Usman, Afolabi Sophiat, Tomori Hammed Babatunde Rasheed Yinka, Adeyi Abdulrasheed, Abdulrazaq Shuaib, and Belgore Abdulrahman, just to mention few, for their sacrifices and moral supports.

DEDICATION

To my parents

ABSTRACT

The use of Micro Gas Turbines (MGTs) is a prominent replacement for electric motors which are commonly used for Unmanned Aerial Vehicles (UAVs) propulsion. MGTs offer better performance than electric motors. For a UAV with relatively high takeoff weight, a MGT will produce more thrust to weight ratio than electric motor. The reason being that the more the thrust required by an electric motor, the larger the battery capacity required to sustain the motor.

The component of the MGT include the inlet, compressor, combustor, and turbine. The design of the compressor, being one of the major components of the MGT, was considered and centrifugal compressor was chosen, among other compressor types, because it delivers high pressure ratio per stage and its operational region.

In designing the centrifugal compressor, literatures on similar work were reviewed during which some important parameters were gathered. The design involves mean line design, which is majorly the application of mathematical equations to check the design result. A Computer Aided Design (CAD) software, CFturbo, which is a design tool for turbo machines was used to obtain the 2D and 3D designs of the compressor. The result of this was validated by comparing the CFturbo design result with that of the mean line design result which showed a good correlation. The performance analysis of the designed compressor was conducted through the application of Computational Fluid Dynamics (CFD). Ansys BladeGen was used to generate the geometry on Ansys and Turbomachinery Fluid Flow, on Ansys, was used to analyze the compressor. The result of the CFD analysis also showed good agreement with that of the mean line design and CFturbo design.

TABLE OF CONTENTS

LIST OF FIGURE

LIST OF TABLES

NOMENCLATURE

CONSTANTS

C_p	Heat capacity at constant pressure = 1.005	[KJ/Kg.K]
γ	Ideal gas constant	[~]
R	Universal gas constant = 287	[J/Kg.K]
Π	pi = 3.142	[rad]

SYMBOLS

C	Absolute velocity	[m/s]
A	Area	[m^2]
h	Diffuser passage depth	[m]
θ	Direction of flow	[°]
ρ	Fluid density	[Kg/m^3]
b	Impeller channel depth	[m]
d	Impeller eye diameter	[m]
D	Impeller diameter	[m]
U_e	Impeller speed at mean radius eye	[m/s]
U	Impeller speed at tip	[m/s]
η_c	Isentropic efficiency	[~]
M	Mach number	[~]
$\dot{m}$	Mass flow rate	[Kg/s]
r	Mean radius	[m]
Z	Number of vanes	[~]
Ψ	Power input factor	[~]
$\dot{W}$	Power required	[W], [J/s]
l	Pressure loss	[~]
N	Rotational speed	[rpm]
β	Relative flow angle	[°]
V	Relative velocity	[m/s]
σ,σ_s	Slip factor	[~]
a	Speed of sound	[m/s]

P_0	Stagnation pressure	[bar], [N/m^2]
T_0	Stagnation temperature	[K], [$^\circ$C]
P	Static pressure	[bar], [N/m^2]
T	Static temperature	[K], [$^\circ$C]
w	Width	[m]
W	Work done	[J]

SUBSCRIPTS

a,x	Axial component
a	Ambient
r	Radial component
r	Root
t	Tip
w,θ	Whirl component

ABBREVIATIONS

1D	One Dimensional
2D	Two Dimensional
3D	Three Dimensional
CAD	Computer Aided Design
CAE	Computer Aided Engineering
CFD	Computational fluid dynamics
FEA	Finite Element Analysis
MGT	Micro Gas Turbine
RPM	Revolutions per minute
UAV	Unmanned Aerial Vehicle

CHAPTER 1

1.1 INTRODUCTION

Research shows that most Unmanned Aerial Vehicles (UAVs) utilizes electric propulsion systems due to the advantages of electric motor and batteries, *Mohamed Kara Mohamed 2015*. Although, electric powered propulsion system offers the advantages of independence on fuel and mechanical engine, as well as low cost. However, the limitation in the electric energy storage, including a very low cruising speed, low ceiling, low rate of climb and low range are important to consider, as well as some imposed design constraints, *Mohammed H. Sadraey 2013*. In a design report of an Object Dropping UAV with a nose mounted electric motor, *Idris Habeeb 2017*, the major design challenge is high landing gear height which is primarily driven by the propeller tip clearance from ground. This result in the landing gear weight constituting about one-third of the aircraft takeoff weight. The single-spool turbojet engine, usually with centrifugal compressor, is a convenient solution, due to the simplicity of construction, compactness, ease of operation, maintenance and better performance, *Irina-Carmen et al 2016*.

The main advantage of Micro Gas Turbine (MGT) over a pack of batteries lies in the high specific energy potential of the fuel-based systems, *Verstraete D. et al* 2005. MGT also has better performance and higher range of operational speeds (cruise speed, rate of climb and maximum speed) than electric propulsion system. Added to the aforementioned MGT features, MGTs possess higher ceiling, range and endurance, *Mohammed H. Sadraey 2013.* For the electric propulsion system, the propeller rpm has a limit it can attain due to shock wave which adversely affects the propeller efficiency. The propeller tips encounters this shock wave when the aircraft speed is close to Mach 1. In contrast, gas turbines can conveniently attain supersonic speeds.

MGTs are a relatively newly developed propulsion system. MGTs offer several advantages compared to other technologies for small scale power generation which includes: a small number of moving parts, compact size, lightweight, greater efficiency and better performance. Waste heat recovery can also be used with this system to achieve efficiencies greater than 80%. Above all, MGTs has higher power to weight ratio compared to existing or in the nearest future, available batteries thus reducing the overall system weight significantly for missions requiring a high power

output and a long duration, *Verstraete D. et al 2005*. These made MGT a better alternative to be adopted for Unmanned Aerial Vehicles (UAVs) propulsion.

Unmanned Aerial Vehicles (UAVs) can be used in varieties of area such as national security, surveillance, election monitoring, crime fighting, disaster management, and search-and rescue operations. UAVs also has its applications in military, agriculture and mining sectors, *Bosman Botha 2012.*

Various approaches in solving this problem has been identified including mathematical modeling. However, the need to carry out a comparative analysis by running a simulation model instead of solving is need for knowledge enhancement. Unlike mathematical model, which is used in most of the reviewed literatures, simulation model is not solved but is run and the changes of system states can be observed at any point in time. This provides an insight into system dynamics rather than just predicting the output of a system based on specific inputs. For this work, simulation model will be considered as it is not a decision making tool but a decision supporting tool, allowing better informed decisions to be made, *Peer-Olaf et al*. The simulation tool to be considered is a computational fluid dynamic (CFD) software, ANSYS Bladegen and Turbomachinery. The compressor will be designed using a computer aided design (CAD) software, CFTurbo, which is designed majorly for turbo-machineries.

The basic components of a micro gas turbine are: inlet, compressor, combustor and the turbine. Compressor, as one of the major components of the turbine, is of two types; the axial compressor, in which intake and exit of air occurs axially; and the centrifugal compressor, in which the air suction is axial and air exits radially. Centrifugal compressor was considered because it operates most efficiently at medium flow rates and high-pressure ratios, *Meherwan 2003*. The centrifugal compressor also delivers higher pressure ratio per stage. The scope of this project is thus limited to “the design and performance analysis of a centrifugal compressor used in micro gas turbines for UAVs”.

Key-words: Unmanned Aerial Vehicle (UAV), Micro Gas Turbine (MGT), Centrifugal compressor, Impeller, Diffuser, Computational Fluid Dynamics (CFD), and Computer Aided Design (CAD).

1.2 PROJECT OBJECTIVES

The major objective of this project is to design a centrifugal compressor which includes both the impeller and diffuser.

The components to be designed will satisfy the following major design parameters:

1. Mass flow rate = 0.63Kg/s;
2. Pressure ratio = 4;
3. Revolution = 80,000rpm and;
4. Impeller diameter of 110mm.

The design parameters stated above are obtained by taking the average of similar MGT parameters. There are other design constraints that will be subsequently considered and discussed in other chapters. To achieve the desired objective, an action plan was devised as shown in figure 1.1. The action plan depicts the systematic steps to be followed to achieve the desired design. The two dimensional (2D) and three dimensional (3D) designs were achieved through the use of CFTurbo and the performance check was done with Ansys Bladegen and Turbogrid and CFX.

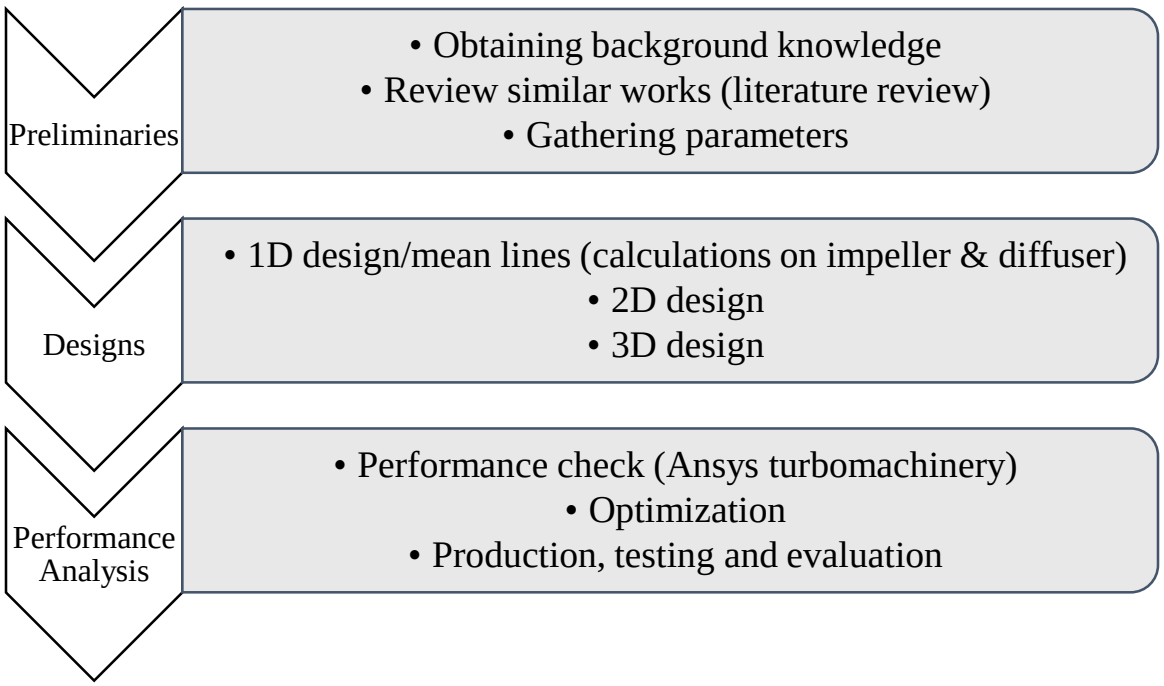

FIGURE 1.1: PROJECT OVERVIEW

1.3 ABOUT COMPRESSORS

A compressor is a device that increases the pressure of a working fluid by reducing its volume. One of the basic aims of using a compressor is to compress the fluid and deliver it at a pressure higher than its original pressure. Compression is required for various purposes, some of which are:

i. To provide air for combustion
ii. To transport process fluid through pipelines
iii. To provide compressed air for driving pneumatic tools
iv. To circulate process fluid through a certain process

Different types of compressors are shown in Figure 1.2. The positive displacement compressors are used for intermittent flow in which successive volumes of fluid are confined in a closed space to increase their pressures. The other broad class of compressors is the rotary type for continuous flow. In this type of compressor, rapidly rotating parts (impellers) accelerate fluid to a high speed; this velocity is then converted into additional pressure by gradual deceleration in the diffuser or volute, which surrounds the impeller, *Meherwan 200.*

The continuous-flow type compressors, as shown in Figure 1.2, can be classified under dynamic or ejector type, entrain the inflowing fluid using a high velocity gas or steam jet, and then convert the velocity of the mixture to pressure in a diffuser. The dynamic compressors have rotating elements, which accelerate the inflowing fluid, and convert the velocity head into pressure head, partially in the rotating elements and partially in the stationary diffusers or blade. The dynamic type can be further subdivided into centrifugal, axial-flow, and mixed-flow compressors. The main flow of gas in the centrifugal compressor is radial. The flow of gas in an axial compressor is axial, and the mixed-flow compressor combines some characteristics of centrifugal and axial compressors, *Meherwan 2003*.

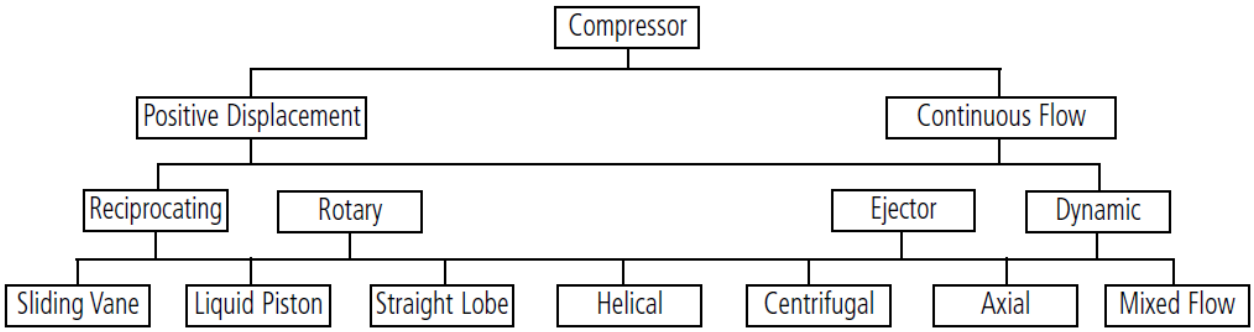

FIGURE 1.2: PRINCIPAL TYPES OF COMPRESSORS

1.3.1 COMPRESSOR SELECTION

The type of compressor required for a certain purpose or application is not always obvious. From the types of compressors mostly used in the process industry, some of the most significant are the centrifugal, axial, rotary, and reciprocating compressors. They fall into three categories as shown in Figure 1.3. For very high flow rates and low-pressure ratios, an axial-flow compressor is the best. An axial compressor usually have a higher efficiency as seen in Figure 1.3, but a smaller operating region than a centrifugal machine. Centrifugal compressor operate most efficiently at medium flow rates and high-pressure ratios. Rotary and reciprocating compressors (positive-displacement machines) are best used for low flow rates and high-pressure ratios. The positive displacement compressors, more commonly known as the reciprocating compressor, were the most widely used compressors in the process and pipeline industries up to and through the 1960s, *Meherwan 2003.*

Upon knowing the selection criteria for each of the compressors, it is important to know their areas of application. For instance, in turbomachinery, the centrifugal flow and axial flow compressors, which are continuous flow compressors, are the ones used for compressing the air. Positive displacement compressors such as the reciprocating, gear type, or lobe type to name just a few, are widely used in the industry for many applications. The characteristics of these compressors are given in table 1.1, *Meherwan 2003*. The pressure ratio of the axial and centrifugal compressors has been classified into three groups: industrial, aerospace and research.

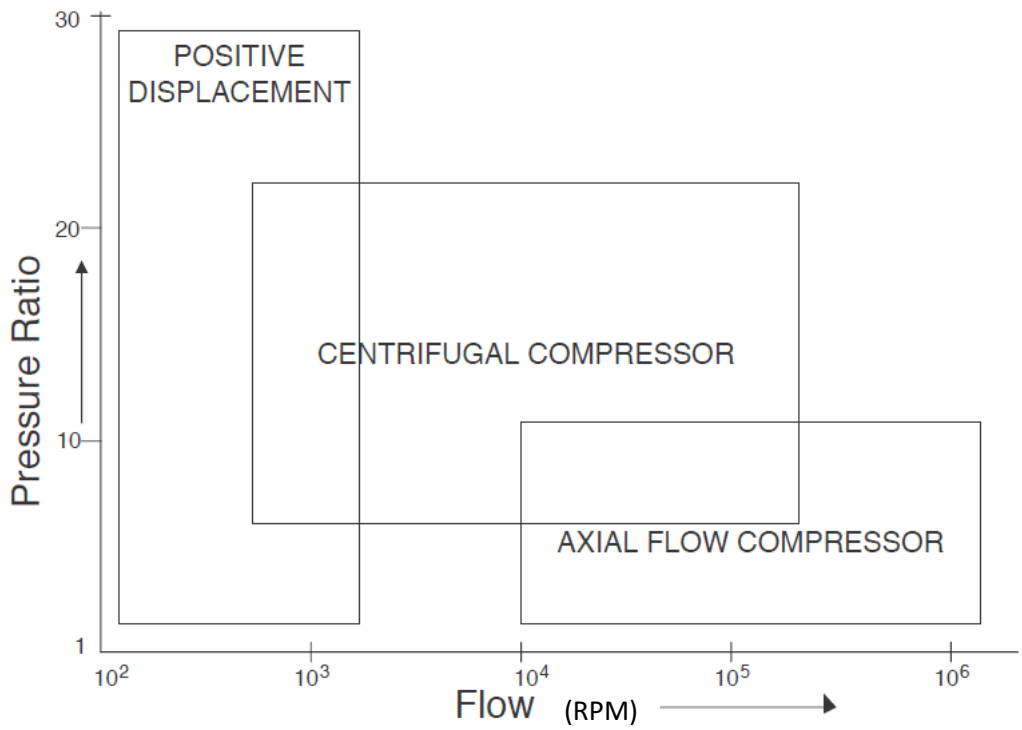

FIGURE 1.3: PERFORMANCE CHARACTERISTICS OF DIFFERENT TYPES OF COMPRESSORS

TYPES OF COMPRESSOR	PRESSURE RATIO			EFFICIENCY	OPERATING RANGE
	Industrial	**Aerospace**	**Research**		
Positive Displacement	Up to 30	–	–	75% – 82%	–
Centrifugal	1.2 – 1.9	2.0 – 7.0	13	75% – 87%	Large 25%
Axial	1.05 – 1.3	1.1 – 1.45	2.1	80% – 91%	Narrow 3% – 10%

TABLE 1.1: COMPRESSOR CHARACTERISTICS

1.3.2 CENTRIFUGAL FLOW COMPRESSOR

Centrifugal compressors are an integral part of the petrochemical industry, finding extensive use because of their smooth operation, large tolerance of process fluctuations, and their higher reliability compared to other types of compressors. They are also used in small gas turbines.

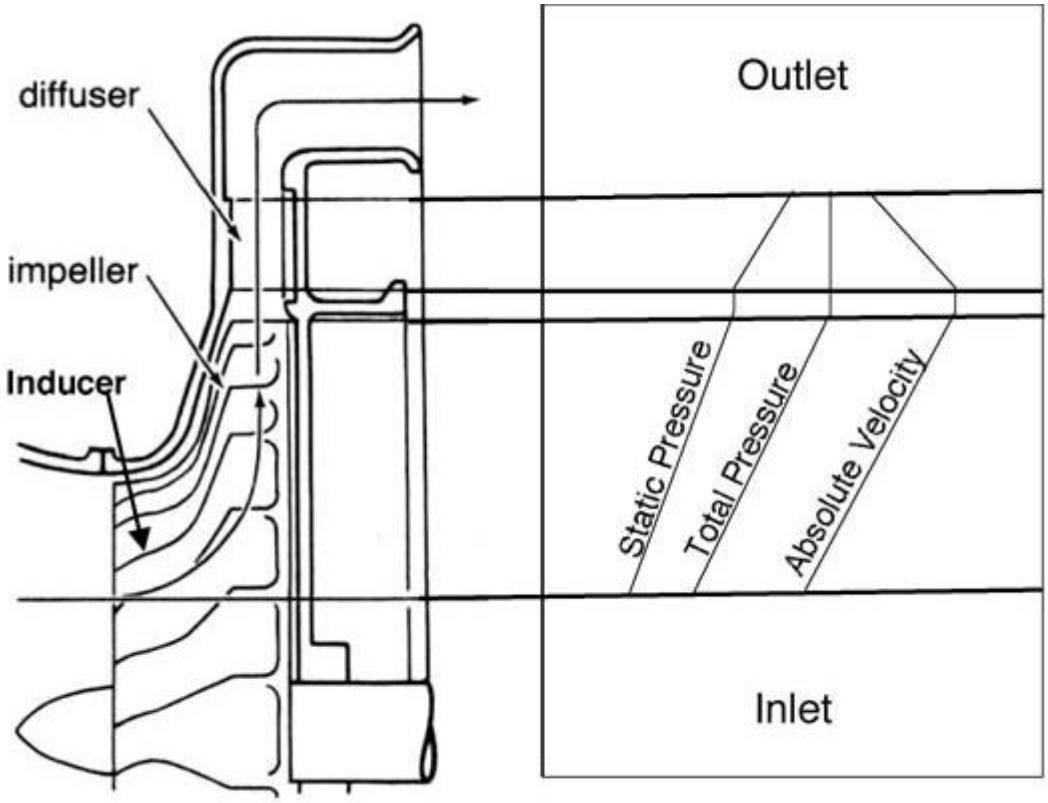

FIGURE 1.4: AERODYNAMIC AND THERMODYNAMIC PROPERTIES IN A CENTRIFUGAL COMPRESSOR STAGE

The operating speed of the centrifugal compressor is high. For aircraft and space application, the rpm can range from 50,000 to 100,000, *Meherwan 2003*. The operation of this centrifugal compressor at various rpm involves moving the fluid through the compressor components. In a typical centrifugal compressor, the fluid enters the compressor in an axial direction and exits in a radial direction. The air initially enters a centrifugal compressor at the inducer, as shown in Figure 1.4. The inducer, usually an integral part of the impeller, is very much like an axial-flow compressor rotor. The fluid is forced through the impeller by rapidly rotating impeller blades. From the inducer, through the impeller, the fluid goes through a 90º turn and exits

into a diffuser, which usually consists of a vaneless space followed by a vanned diffuser. This is especially true if the compressor exit is supersonic, as is the case with high-pressure ratio compressors.

In a diffuser with vaneless space before the vanned region, the vaneless space is used to reduce the velocity leaving the rotor to a value lower than Mach 1 (M<1). The velocity of the fluid is converted to pressure, partially in the impeller and partially in the stationary diffusers. Most of the velocity leaving the impeller is converted into pressure energy in the diffuser as shown in Figure 1.4. It is normal practice to design the compressor so that half the pressure rise takes place in the impeller and the other half in the diffuser. The diffuser consists essentially of vanes, which are tangential to the impeller. These vane passages diverge to convert the velocity head into pressure energy. The inner edge of the vanes is in line with the direction of the resultant airflow from the impeller, as shown in Figure 1.5. This combination of rotor (or impeller) and diffuser comprises a single stage, *Meherwan 2003*.

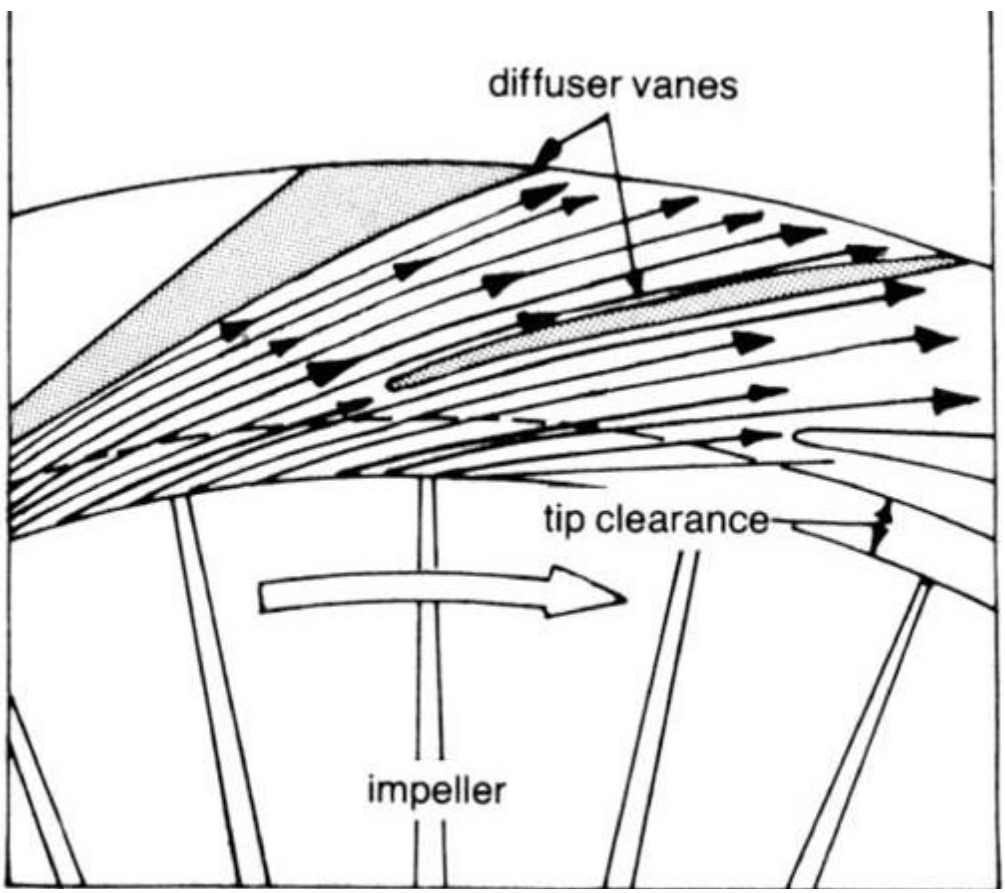

FIGURE 1.5: FLOW IN A VANNED DIFFUSER

CHAPTER 2

2.1 LITERATURE REVIEW

This chapter entails both a summary and explanation of the complete and current state of knowledge on the design and analysis of a Centrifugal compressor for a MGT used in UAVs as found in academic books and journal articles. This literature review will focus on three areas, namely MGT, CFD and review of similar works on this topic.

2.2 MICRO GAS TURBINES

The physics behind the operation of MGTs and larger turbomachines of the same type (axial or radial) are essentially the same. However, applying scaling procedures to large, existing turbomachinery components in order to design MGTs presents some problems, *Bosman Botha 2012*. According to Van den Braembussche (2005), the following are the main issues:

i. The large difference in Reynolds number between large and micro gas turbomachinery components.

ii. Significant heat transfer between the hot and cold components in micro turbomachinery which is negligible in large machines

iii. Geometrical and mechanical restrictions incurred by the manufacturing processes and mechanical properties of micro turbomachinery components.

Conserving the thermodynamic cycle characteristics is the first requirement when scaling a gas turbine. This implies the same energy exchange between fluid and rotating components but at a smaller mass flow rate, *Van den Braembussche 2005*.

According to the Scientific Conference on Automotive Vehicles and Combustion Engines in 2016, Construction of contemporary MGTs as well as turboshaft and turbojet ones is the result of about twenty years of development of that idea. Interesting is that the first designs were done by a group of enthusiasts of aviation model making. There was the need of finding of real engines, but made in micro scale, for propulsion of turbojet or turboprop aircraft models. The development of that area has been the object of particular interest of army. The idea of micro turbine engines application to the propulsion of small and medium size “professional” military Unmanned Aerial Vehicles (UAVs) is, at present, highly developed. On the base of market demand many specialized

firm manufacturing different kinds of micro turbine engines have been established in the world. There are several concepts of construction of mentioned engines depending on the custom demands and available know-how. The selected examples of contemporary micro turbine engines, illustrating contemporary state of art within this area are presented below.

2.3 COMPUTATIONAL FLUID DYNAMICS

The development of computer fluid dynamics has been closely associated with the evolution of large high-speed computers. At first the principal incentive was to produce numerical techniques for solving problems related to national defense. Soon, however, it was recognized that numerous additional scientific and engineering applications could be accomplished by means of modified techniques that extended considerably the capabilities of the early procedures, *Francis H. Harlow, 2003*.

Computational Fluid Dynamics (CFD) is a numerical technique used for the solution of the equations governing fluid flow and heat transfer problems inside a defined flow geometry, *Ghani Albaali 2006*. It is a methodology for obtaining discrete solution of real world fluid problems. Discrete solution is a solution obtained at a finite collection of space points and at discrete time levels. For a reasonably accurate solution, the number of space points that need to be involved is of the order of few millions, *IIT Kanpur 2016*. The higher the space points, the more accurate is the solution.

CFD is a tool for compressing the design and development cycle allowing for rapid prototyping. It has the benefits of better insight (more details), foresight (better prediction, in a short time) and efficiency (i.e. better and faster design). This enables designer to meet environmental regulations and ensure industry compliance. CFD analysis leads to shorter design cycles and products get to market faster, *IIT Kanpur 2016*.

CFD encompasses simulation-based design instead of “build & test” and simulation of physical fluid phenomena that are difficult for experiments. Examples of this include full scale simulation (e.g. engines, airplanes, ships, etc.), environmental effects (e.g. wind, weather, etc.), hazards (e.g. explosions, radiation, pollution, etc.), physics (e.g. planetary boundary layer, stellar evolution), etc., *IIT Kanpur 2016*.

2.3.1 CFD PROGRAM

The use of CFD techniques to solve a fluid flow and heat transfer problems is split into three discrete parts: *preprocessing*, *processing* and *post processing*. In general, different computer programs that form the CFD code must undertake each of the three tasks, *Ghani Albaani 2006*.

2.3.1.1 Definition of a CFD Problem (Preprocessor)

The first stage in solving a CFD problem is to define all the relevant parameters required by the CFD code prior to the numerical solution process, as follows:

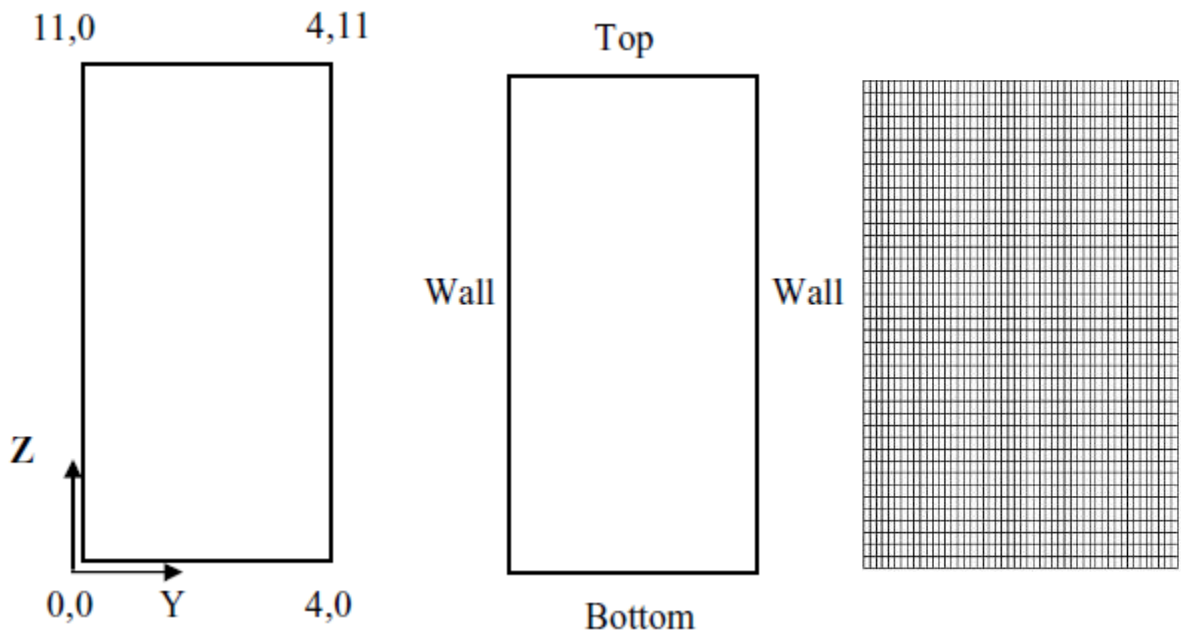

(A) (B) (C)

FIGURE 2.1: (A) DEFINITION OF CFD GEOMETRY (B) DEFINITION OF BOUNDARY CONDITIONS (C) MESH BUILDING

1. Definition of physical geometry of the environment in which the fluid flows. This is usually done by creating a geometry to represent the environment. It can be the creation of the problem domain that needs to be analyzed.
2. Definition of boundary conditions of the defined environment. The conditions included the definition of some areas such as inlets and outlets for the fluid flow and the boundary areas of solids where heat transfer from or to the fluid can occur.

3. Construction of mesh or grid as a geometric representation of the physical environment. This mesh or grid will form the computational grid that will be used in the solution of the problem by the mathematical technique around which CFD is based.

2.3.1.2 Solution of the Problem (Processor)

The solution of the problem by the CFD code is where a host of mathematical techniques is used to approximate the differential equations into algebraic form, which can be solved directly or iteratively. Different CFD codes employ different solution techniques, but the physics is the same if it can be well defined and understood. The solution of the transport equations for the geometry under study is not a trivial matter and cannot be solved readily, if at all, by analytical techniques. CFD uses numerical techniques to solve discretized representations of the transport equations.

Direct or explicit numerical methods, which can be both extremely accurate and rapid, may be used if sufficient computing power is available. Many codes use iterative methods to solve the equations because they tend to be more robust, although they can take longer to converge. Standard texts are available that provide good background material on numerical simulation and CFD, *Ghani Albaani 2006*.

2.3.1.3 Analysis of Result (Postprocessor)

The results can be analyzed both numerically and graphically. The postprocessor takes the numerical results and displays them as a visual representation. It displays a visual image of the physical geometry through which the fluid flows, with the option of printing a hard copy of all the results as tables of numbers and other means. It is possible to superimpose the velocity, pressure, and temperature distributions within the fluid. The format of this display is a graphical contour with the option of displaying scaled arrows for vector quantities. The output file can contain all sorts of information, including the spatial coordinates of all of the cells in the computational mesh and the solved transport variables for each cell. In the case of a large CFD problem, say greater than 100,000 cells, it is obvious that the user does not want to read through this file. Thus, the second method offers the user the ability to visualize the results. This method, often referred to as post processing, takes the results from the CFD solver and allows the user to display variables graphically on the computer screen, for all or part of the flow domain. These graphical

representation methods include vector plots (a scaled arrow pointing in the direction of flow), contour plots on a two-dimensional (2-D) slice through the domain, and iso-surface plots (a 3-D surface on which a variable is constant). The user has the option to rotate the image in 3-D space or to zoom into areas of interest to extract the most useful information from the image. Combining both visual and numerical results allows the optimal solution to be achieved for the problem under investigation, *Ghani Albaani 2006*.

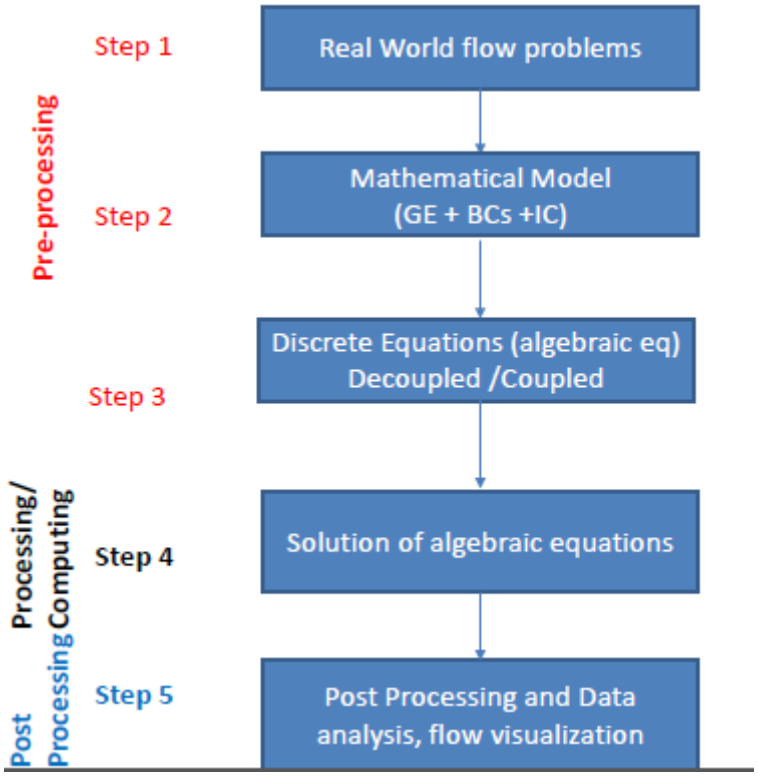

FIGURE 2.2: STEPS IN CFD ANALYSIS

2.3.2 CFD APPLICATION

According to Ghani Albaani, in 2006, CFD has wide range of applications in the areas of fluid and heat transfer within the aerospace and nuclear industries backed by the availability of powerful supercomputers. CFD has its application in vast areas some of which are aerospace, automotive, biomedical, chemical processing, hydraulics, marine, oil and gas, power generation, sport, etc., *IIT Kanpur 2016*.

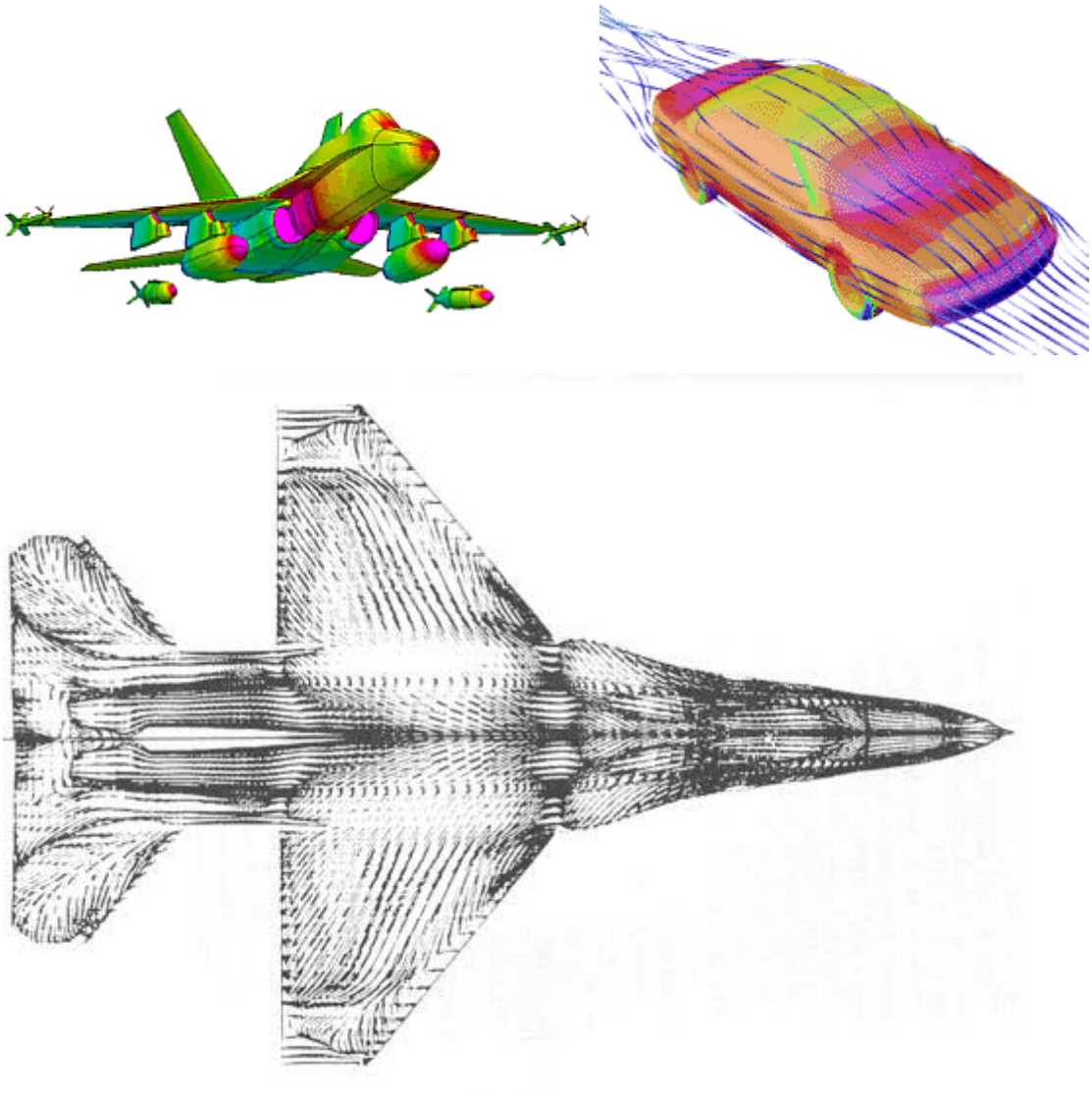

FIGURE 2.3: APPLICATION OF COMPUTATIONAL FLUID DYNAMICS

2.4 PREVIOUS WORKS ON DESIGN AND ANALYSIS OF CENTRIFUGAL COMPRESSOR

Research into the design and performance analysis of centrifugal compressor for MGTs used in UAVs is not new entirely. Several works, similar to this project, has been done earlier. In *2012*, *Bosman* worked on the Design of a centrifugal compressor impeller for MGT application. *Vijaykumar, in 2007,* performed an illustration of the design methodology for aerodynamic design of centrifugal compressor. *Ismail et al* worked on the aerodynamic design of small radial compressors in 1998. The design and optimization of a mixed flow compressor impeller using

robust technology for a small turbo jet engine was done by *Cevik in 2009*. And *Irina-Carmen et al* studied the use of turbojet engines for UAVs in *2016*.

In *2018, Mayowa* designed a centrifugal compressor impeller and devised a methodology and tools with which to perform the aforementioned. The compressor impeller designed adhered to the specific performance and dimensional requirements. The new compressor was designed using a mean-line performance calculation code and compared with that of the design tool – CFTurbo. According to the CFD result, the final design delivered good performance at the design speed with regards to pressure ratio, efficiency, and stall margin. *B. B. Van der Merwe* also designed a centrifugal compressor impeller during which befitting methodology and required tool was devised to achieve the desired design. The code used wan vindicated through comparison with the results from a benchmark study. This comparison included mean-line, CFD, and experimental results: the new design mean –line results were compared to the results of CFD simulations performed on the same design. The new design was optimized using an Artificial Neural Network (ANN) and Genetic Algorithm. Prior to and during optimization, the ANN was trained using a database of sample CFD calculations. A Finite Element Analysis (FEA) was done on the optimized impeller geometry to ensure that failure would not occur during operation. According to CFD results, the final design delivered good performance at the design speed with regards to pressure ratio, efficiency and stall margin. The mechanical stresses experienced during operation were also within limits. Experimental results showed good agreement with CFD results of the optimized impeller.

In an effort to reduce fuel consumption and remain competitive in an automotive industry that continues to increase regulations for environmental protection, there has been an increase in the use of turbochargers. Due to this increase in demand, *Xavier Medina et al, in 2014*, studied the optimization of centrifugal compressor that provides a wide and stable operating range that delivers a high-pressure output at a competitive price. The analysis of the phenomena that occurs within a centrifugal compressor is extremely challenging and presents three-dimensional unsteady flow analysis with the addition of thermal flow and expansion. Based on experimental and numerical simulation analysis, this team developed a blade design for a centrifugal compressor using computational optimization methods. The ultimate goal of this project is to create a blade design that results in a wider optimum operating range whilst increasing the pressure ratio without decreasing the mass flow rate that the engine requires for stable combustion.

As far back as *1967, A. D. Welliver et al* researched into the analysis and experimental evaluation to define the design criteria and performance characteristics of the high pressure ratio single stage centrifugal compressor. The overall performance target was a pressure ratio of 10:1 at an adiabatic efficiency of 80 percent at an airflow of 2 pounds per second. The research led to development of advanced technologies applicable to MGTs.

Mayowa, in 2017, studied the development of a design optimization methodology that could generate an optimum centrifugal compressor impeller design. The methodology covers the design process from initial conceptual phases, to the end of the preliminary design phase. Design studies in the literature generally focus on the detailed design process which mostly involves CFD solutions and their validations. The information available on how to design and optimize a compressor from beginning to the end of the design process wasn't sufficient. Therefore, the study concentrates on converting, relating and reflecting the basic performance requirements of a small gas turbine engine to the design of the compressor through a robust design optimization procedure.

In *2009, Cevik Mert's* study focused on developing an individual design methodology for a centrifugal impeller and generating a mixed flow impeller for a small turbojet engine with the use of this methodology. The structure of the methodology is based on the design, modeling and the optimization processes, which are operated sequentially. The design process consists of engine design and compressor design codes operated together with a commercial design code. Design of Experiment methods and an in-house Neural Network code is used for the modeling phase. The optimization is based on an in-house code which is generated based on multidirectional search algorithm. The optimization problem is constructed by using the in house parametric design codes of the engine and the compressor. The goal of the optimization problem is to reach an optimum design which gives the best possible combination of the thrust and the fuel consumption for a small turbojet engine.

A one dimensional (mean-line) design methodology for a medium pressure ratio Centrifugal Compressor was done by *Anand Vijaykumar in 2007*. A computational procedure for design of a Centrifugal Compressor was established. The numerical model is based on the conservation principles of mass, momentum and energy conservation and has been utilized to predict the operational and aerodynamic characteristics of a small centrifugal compressor as well as determining the performance and geometry of compressor blades, both straight and backswept. The design code provided a basis on which the design of the Compressor can be modeled by

varying the key parameters which include both aerodynamic and geometric details. The code then predicted and gave a first cut solution, which further helped in zeroing on to a particular design for the given requirements. The design which models the flow in an Impeller, Diffuser and an annular bend takes into consideration various loss models occurring in the complex flow of a Centrifugal Compressor. It makes use of a Jet-Wake Model i.e. it splits the flow into Primary and Secondary zone and performs a Mixed flow Analysis. The Design also performed an inverse flow analysis wherein we get the geometry by specifying aerodynamic details. The design has been exhaustively validated by using a number of Test Compressors from NASA test reports. Based on the geometry computed by the code, an impeller model is generated using ANSYS BLADEGEN-Tool.

L. C. B. de Villiers worked on a detailed methodology for developing a centrifugal compressor for application in a Micro Gas Turbine (MGT) in *2014*. This research forms part of a larger project, namely project Ballast, initiated by the South African Air Force (SAAF) in conjunction with Armscor. The methodology encompasses the development of a mean-line code that makes use of 1-dimensional theory in order to create an initial centrifugal compressor geometry which includes a rotor as well as radial vanned diffuser. This is followed by a Computational Fluid Dynamics (CFD) simulation process during which the compressor was optimized in order to maximize its performance. Before manufacturing a Finite Element Analysis (FEA) was done in order to ensure that the rotor does not fail during testing. The testing of the compressor is done to compare the numerical results with the experimental results and in so doing confirms the design process.

K. A. R. Ismail et al researched on a computational procedure for the analysis of steady one-dimensional centrifugal compressor. The numerical model is based on the conservation principles of mass, momentum and energy, and was utilized to predict the operational and aerodynamic characteristics of a small centrifugal compressor as well as determining the performance and geometry of compressor blades, both straight and curved.

CHAPTER 3

3.1 DESIGN OBJECTIVE

The objective is to design a centrifugal compressor for a MGT which is to be used in a UAV. The compressor components to be designed are impeller and diffuser.

Design studies in this project report generally focus on the detailed design process which mostly involve CAD and CFD analysis. The objective also include the validation of the CAD through comparison with mean-line design.

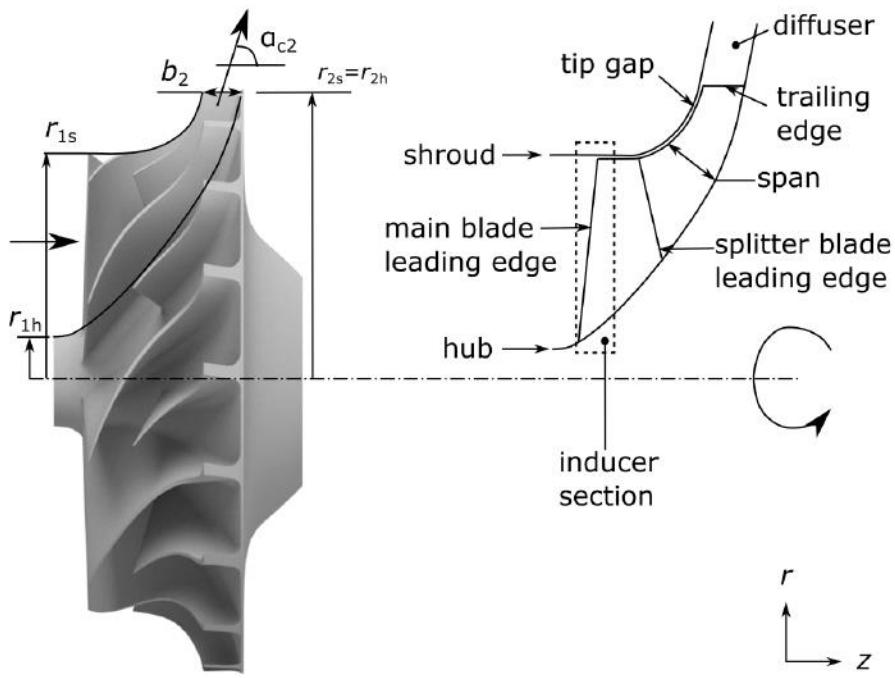

FIGURE 3.1: COMPRESSOR COMPONENTS IN THE MERIDIONAL PLANE

3.2 DESIGN OVERVIEW

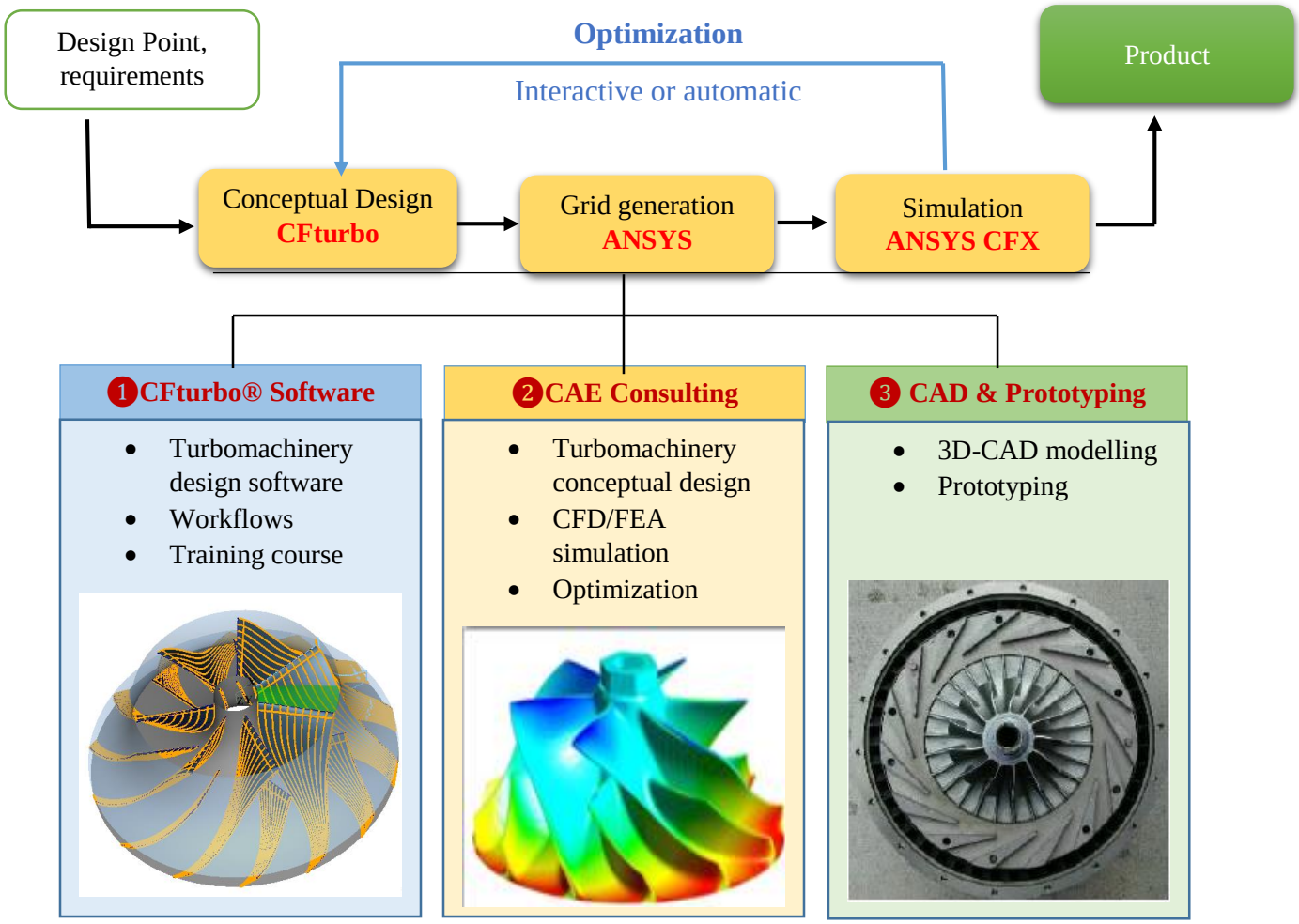

FIGURE 3.2: DESIGN OVERVIEW

3.3 DESIGN SPECIFICATIONS

The following data are considered as a basis for the design of the centrifugal compressor:

1. Speed – 80,000rpm
2. Impeller diameter – 110mm
3. Pressure ratio – 4
4. Mass flow rate – 0.63Kg/s
5. Isentropic efficiency – 0.78
6. Power input factor, Ψ – 1.04
7. Slip factor, σ – 0.9
8. Eye tip diameter, d_t – 80mm
9. Eye root diameter, d_r – 18mm
10. Inlet stagnation temperature, T_{01} – 293K (20C)
11. Inlet stagnation pressure, P_{01} – 1bar (101325N/m^2)
12. Radial width of vaneless space, w_{vl} = 11mm
13. Approximate mean radius of diffuser throat, r_t = 91mm
14. Depth of diffuser passage, h_2 = 25mm
15. Number of diffuser vanes, Z_d = 26

These parameters were obtained by considering that of other similar designs.

3.4 DESIGN METHODOLOGY

This section covers the description of the work done. In designing the impeller and diffuser, three aspects were considered, before analysis. The aspects are:

1. One dimensional (1D) design/mean line design (Calculations)
2. Two dimensional (2D) design
3. Three dimensional (3D) design

The 1D design or mean line design was carried out through the use of governing mathematical equations.

F	G	H	I	J	K	L	M	N	O	P	Q	R	S	T
IMPELLER DESIGN														
Pressure ratio and power required				Iteration for C1				Flow at inducer				Impeller Width at Exit		
Parameters	Unit	Value		Parameter	Unit	Value		Parameter	Unit	Value		Parameter	Unit	Value
U	m/s	460.8266667		A1	m^2	0.006408		Ur	m/s	75.408		P2/P01	1	2.5154817
T03 - T01	K	197.7811929		ρ1	Kg/m^3	1.189188		Ut	m/s	385.8376		P2	Pa	2.52E+05
P03/P01	1	4.194263458		Ca1	m/s	82.66818		βr	deg	48.51773		ρ2	Kg/m^3	2.182534
Power	W	125225.1623						βt	deg	12.46376		A	m^2	0.00338534
				Dynamic t	K	3.400014						b	m	0.00979497
				T1	K	289.6		Absolute Velocity at exit						
				P1	Pa	95997.12		Cr2	m/s	85.26629		x	y	
				ρ1	Kg/m^3	1.154989		Cw2	m/s	414.744		0	0	
				Ca1	m/s	85.11597		Dyn. Tem	K	89.19549		0	37.05	
												43.8	37.05	
				Dynamic t	K	3.604343		Distribution of Loss				43.8	54.35	
				T1	K	289.3957		l	1	0.125		51.4	54.35	
				P1	Pa	95760.27		P02/P01	1	5.075806		51.4	0	
				rho1	Kg/m^3	1.152953		T02=T03	K	490.7812		0	0	
				Ca1	m/s	85.26629		T2	K	401.5857				
								P2/P02	1	0.495583				
				Dynamic t	K	3.617085						Estimation of number of blades		
				T1	K	289.3829						Z	1	19.7946
				P1	Pa	95745.51								
				rho1	Kg/m^4	1.152826								
				Ca1	m/s	85.27568								

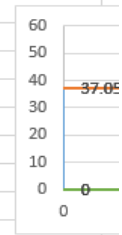

DIFFUSER DESIGN										
Radial Velocity				Static Density a Diffuser Inlet				Diffuser Inlet Angle		
Parameter	Unit	Value		Paramete	Unit	Value		Paramete	Unit	Value
r2	m	0.066		T2	K	431.1305		A	m^2	0.010369
Cw2	m/s	345.62		P2/P02	1	0.635364		Cr2	m/s	23.3122
A2	m^2	0.013686552		P2/P01	1	3.224985		β	deg	3.859062
ρ2	Kg/m^3	2.182534		P2	Pa	3.22E+05				
Cr2	m/s	21.0904322		ρ2	K/m^3	2.606376		atic Density at Diffuser Thro		
C2^2/2Cp	K	59.65074166						Cw2	m/s	250.6695
Po2/Po1	1	5.075805678						Cr2	m/s	14
								C2^2/2Cp	K	31.35879
								T2	K	459.4224
Diffuser Angle at Throat				nducer Relative Mach on Groun				P2/P02	1	0.793661
Ar2	m^2	0.0142961		Inlet Velo	m/s	85.26629		P2/P01	1	4.028468
Cr2	m/s	14.42371582		Eye tip sp	m/s	385.8376		p2	Pa	4.03E+05
Flow directi	deg	3.293455112		Vt	m/s	395.1468		ρ2	K/m^3	3.055243
				a	m/s	343.1143				
Diffuser Throat Width				Max Mach	1	1.151648				
A2	m^2	0.00082125								
b2	m	0.001263462								

FIGURE 3.3: 1D DESIGN/MEAN LINE DESIGN. ADAPTED FROM EXCEL SPREADSHEET

A turbomachinery CAD software, CFturbo, was used to design the impeller and diffuser in 2D and 3D. The result of this was validated by comparing it with that of the mean line design.

CFD analysis was then performed on the CFturbo design through simulation with ANSYS Turbomachinery.

ANSYS Turbomachinery is a simulation tool for turbo machines. Mesh generation using this tool is to be done by “Turbogrid” which recognizes the inlet, outlet, and flow domain by default. The “solution” in this tool utilizes “ANSYS CFX” which serves the purpose of the solver and the “result” utilizes “CFD Post”.

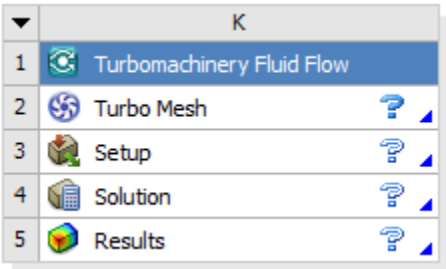

FIGURE 3.4: ANSYS TURBOMACHINERY FLUID FLOW

3.4.1 MEAN-LINE ANALYSIS

This section discusses the equations used in the design of the impeller and diffuser.

3.4.1.1 DESIGN PROCEDURE

- Assume rotational speed, tip speed, and air entry velocity
- Determine the pressure ratio of the compressor and the power required to drive it, assuming that the velocity of the air at inlet is axial
- Calculate the inlet angle of the impeller vanes at the root and tip radii of the eye assuming that the axial inlet velocity is constant across the eye
- Estimate the number of vanes
- Estimate the axial depth of the impeller channels at the periphery of the impeller
- Estimate the inlet angle of the diffuser vanes and the throat width of the diffuser passage, which are assumed to be of constant depth.

The design specifications have been stated earlier (section 3.3).

3.4.1.2 DESIGN REQUIREMENTS

The design requirements are:

- To determine the pressure ratio of the compressor and the power required to drive it assuming that the velocity of the air at inlet is axial
- To calculate the inlet angle of the impeller vanes at the root and tip radii of the eye, assuming that the axial inlet velocity is constant across the eye
- To estimate the axial depth of the impeller channels at the periphery of the impeller

3.4.1.3 DESIGN FORMULAE

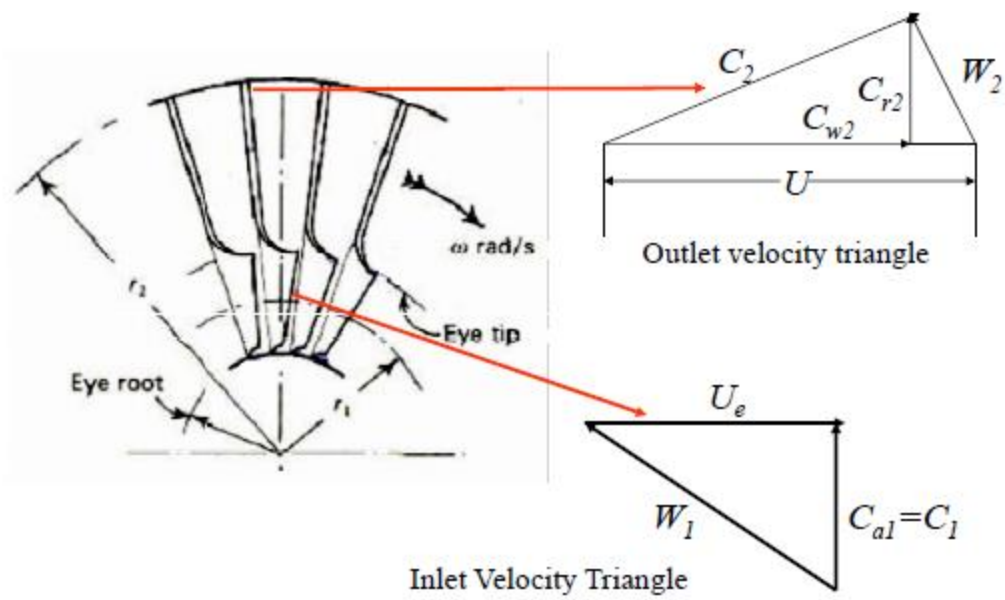

FIGURE 3.5: VELOCITY TRIANGLE

From Euler turbine equation of energy exchange, the specific work is expressed as:

$$\dot{W} = \left(U_2 C_{w_2} - U_e C_{w_1}\right) = h_{03} - h_{01} \quad (3.1)$$

$$W = c_p(T_{03} - T_{01}) \quad (3.2)$$

If the flow at the inlet to the impeller is axial, then $C_{w_1} = 0$ and

$$\dot{W} = U_2 C_{w_2} = c_p(T_{03} - T_{01}) \quad (3.3)$$

Slip factor, $\sigma = \frac{C_{w_2}}{U_2}$ (3.4)

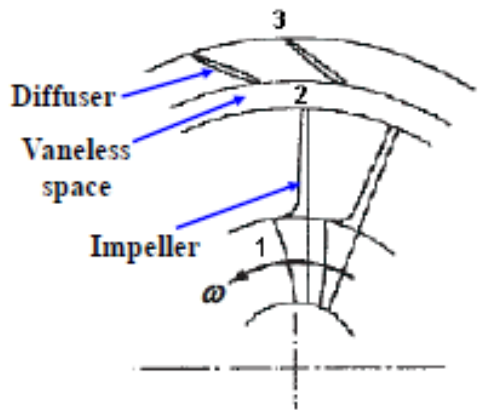

FIGURE 3.6: COMPRESSOR REGIONS

Then, $\dot{W} = \sigma {U_2}^2$ (3.5)

Introducing the power input factor, Ψ,

$\dot{W} = \Psi \sigma {U_2}^2$ (3.6)

3.4.1.3.1 IMPELLER DESIGN FORMULAE

<u>Pressure ratio and power required</u>

Impeller tip speed, $U = \pi D N$ (3.7)

$T_{03} - T_{01} = \frac{\Psi \sigma {U_2}^2}{C_p}$ (3.8)

$$\frac{P_{03}}{P_{01}} = \left(\frac{T_{03}}{T_{01}}\right)^{\frac{\gamma}{\gamma-1}} = \left[1 + \frac{\eta_c (T_{03} - T_{01})}{T_{01}}\right]^{\frac{\gamma}{\gamma-1}}$$

$$= \left[1 + \frac{\eta_c \Psi \sigma {U_2}^2}{c_p T_{01}}\right]^{\frac{\gamma}{\gamma-1}} \quad (3.9)$$

Power required,

$\dot{W} = \dot{m}\, c_p (T_{03} - T_{01})$ (3.10)

<u>Iteration on C_{a1}</u>

Annulus area of impeller eye,

$A_1 = \frac{\pi (d_t^2 - d_r^2)}{4}$ (3.11)

Based on stagnation conditions,

$$\rho_1 \cong \frac{P_{01}}{RT_{01}} \tag{3.12}$$

From continuity equation,

$$C_{a1} = \frac{\dot{m}}{\rho A_1} \tag{3.13}$$

Since $C_1 = C_{a1}$, the equivalent dynamic temperature is $\frac{C_1^2}{2c_p}$

$$T_1 = T_{01} - \frac{C_1^2}{2c_p} \tag{3.14}$$

$$P_1 = \frac{P_{01}}{(T_{01}/T_1)^{\gamma/(\gamma-1)}} \tag{3.15}$$

$$\rho_1 = \frac{P_1}{RT_1} \tag{3.16}$$

Iterations were then carried out between equations (3.13) and (3.16) until C_{a1} converges and the deviation is within a reasonable convergence criterion of about 10^{-3}.

<u>Flow angles at inducer</u>

Peripheral speed at the impeller eye tip radius,

$$U_t = \pi d_t N \tag{3.17}$$

And the root radius,

$$U_r = \pi d_r N \tag{3.18}$$

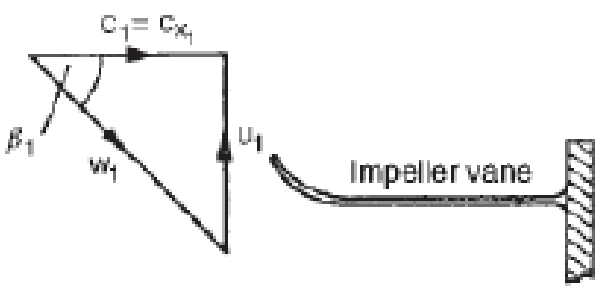

FIGURE 3.7: FLOW ANGLES AT INDUCER

At root and tip, the flow angles are respectively:

$$\beta_r = \tan^{-1}\left({C_{a1}}/{U_r}\right) \tag{3.19}$$

$$\beta_t = \tan^{-1}\left({C_{a1}}/{U_t}\right) \tag{3.20}$$

Absolute velocity at exit

Deciding that $C_{r2} = C_{a1}$

$$C_{w2} = \sigma U \tag{3.21}$$

$$\frac{C_2^2}{2c_p} = \frac{C_{r2}^2 - C_{w2}^2}{2c_p} \tag{3.22}$$

Distribution of total loss

Making an assumption that half of the total loss occurs in the impeller,

$$l = 0.5(1 - \eta_c) \tag{3.23}$$

$$\frac{P_{02}}{P_{01}} = \left[1 + \frac{(1-l)\times(T_{03} - T_{01})}{T_{01}}\right]^{\frac{\gamma}{\gamma-1}} \tag{3.24}$$

$$T_{02} = T_{03} = (T_{03} - T_{01}) + T_{01} \tag{3.25}$$

$$T_2 = T_{02} - \frac{C_2^2}{2c_p} \tag{3.26}$$

For an isentropic flow,

$$\frac{P_2}{P_{02}} = \left(\frac{T_2}{T_{02}}\right)^{\frac{\gamma}{\gamma-1}} \tag{3.27}$$

Impeller width at exit

$$\frac{P_2}{P_{01}} = \frac{P_2}{P_{02}} \cdot \frac{P_{02}}{P_{01}} \tag{3.28}$$

$$P_2 = \frac{P_2}{P_{01}} \times P_{01} \tag{3.29}$$

$$\rho_2 = \frac{P_2}{RT_2} \tag{3.30}$$

The required flow area normal to the radial direction at impeller tip is:

$$A = \frac{\dot{m}}{\rho_2 C_{r2}} \tag{3.31}$$

Hence, the depth of the impeller channel at exit is:

$$b = \frac{A}{\pi D} \tag{3.31}$$

Estimation of number of blades

The number of impeller vanes can be obtained from the correlations for slip factor:

Stanitz correlation

$$\sigma_s = 1 - \frac{0.63\pi/Z}{1-\phi_2 \tan \beta_2'} \quad (3.32)$$

Stodola Correlation

$$\sigma = 1 - \frac{(\pi/Z)\cos \beta_2'}{1-\phi_2 \tan \beta_2'} \quad (3.33)$$

Wiesner Corellation

$$\sigma_s = 1 - \frac{\sqrt{\cos \beta_2}}{Z^{0.7}} \quad (3.34)$$

Where,

$$\phi_2 = C_{r2}/U_2 \quad (3.35)$$

and β_2' is measured from radial direction.

In the present case, $\beta_2' = 0$

Hence, stanitz correlation reduces to

$$\sigma_s = 1 - \frac{0.63\pi}{Z} \quad (3.36)$$

Impeller design result

Considering the design specifications stated in section 3.3, the table below shows the mean-line impeller design results.

IMPELLER DESIGN			
Design Specifications			
S/N	Parameters	Unit	value
1	Power input factor, Ψ	1	1.04
2	Slip factor, σ	1	0.9
3	Rotational speed, N	rev/s	1333.333
4	Impeller dia (D)	m	0.11
5	Mass flow rate	Kg/s	0.63
6	Eye tip dia, d_t	m	0.0921
7	Eye root dia, d_r	m	0.018
8	Temp, T_{01}	K	293
9	Pressure, P_{01}	Pa or N/m^2	1.00E+05
10	Isentropic efficiency, n_c	1	0.75

Constants			
11	Cp	J/Kg K	1005
12	γ	1	1.4
13	R	J/Kg K	287
14	π	rad	3.142
Pressure ratio and power required			
15	Parameters	Unit	Value
16	U	m/s	460.8266667
17	T_{03} - T_{01}	K	197.7811929
18	P_{03}/P_{01}	1	4.194263458
19	Power	W	125225.1623
Iteration for C1			
	Parameter	Unit	Value
20	A_1	m^2	0.006408
21	ρ_1	Kg/m^3	1.189188
22	C_{a1}	m/s	82.66818
Iteration 1			
	Dynamic temp.	K	3.400014
23	T_1	K	289.6
24	P_1	Pa	95997.12
25	ρ_1	Kg/m^3	1.154989
26	C_{a1}	m/s	85.11597
Iteration 2			
	Dynamic temp.	K	3.604343
27	T_1	K	289.3957
28	P_1	Pa	95760.27
29	ρ_1	Kg/m^3	1.152953
30	C_{a1}	m/s	85.26629
Iteration 3			
	Dynamic temp.	K	3.617085
31	T_1	K	289.3829
32	P_1	Pa	95745.51
33	ρ_1	Kg/m^3	1.152826
34	C_{a1}	m/s	85.27568
Flow at inducer			
	Parameter	Unit	Value
35	U_r	m/s	75.408
36	U_t	m/s	385.8376

37	β_r	deg	48.51773
38	β_t	deg	12.46376
Absolute Velocity at exit			
39	C_{r2}	m/s	85.26629
40	C_{w2}	m/s	414.744
41	Dynamic Temperature	K	89.19549
Distribution of Loss			
42	l	1	0.125
43	P_{02}/P_{01}	1	5.075806
44	$T_{02}=T_{03}$	K	490.7812
45	T_2	K	401.5857
46	P_2/P_{02}	1	0.495583
Impeller Width at Exit			
	Parameter	Unit	Value
47	P_2/P_{01}	1	2.5154817
48	P_2	Pa	2.52E+05
49	ρ_2	Kg/m^3	2.182534
50	A	m^2	0.003385339
51	b	m	0.009794974
Estimation of number of blades			
52	Z	1	19.7946

TABLE 3.1: MEAN LINE IMPELLER DESIGN RESULT

3.4.1.3.2 DIFFUSER DESIGN FORMULAE

<u>Radial velocity at diffuser inlet</u>

Radius of the diffuser vane leading edge,

$$r_2 = \left(w_{v_l} + \frac{D}{2}\right) \tag{3.37}$$

$$C_{w2_{new}} = C_{w2} \times \frac{D/2}{r_2} \tag{3.38}$$

$$A_2 = \pi r_2^2 \tag{3.39}$$

$$\rho_2 = \frac{P_2}{RT_2} \tag{3.40}$$

$$C_{r2} = \frac{\dot{m}}{\rho_2 A_2} \tag{3.41}$$

$$\frac{C_2^2}{2C_p} = \frac{C_{r2}^2 + C_{w2}^2}{2c_p} \tag{3.42}$$

Iterate within the equations until it converges.

Ignoring any additional loss between the impeller tip and the diffuser vane leading edge, the stagnation pressure will be that calculated for the impeller tip, P_{02}/P_{01}.

Static density at diffuser inlet

Proceeding as before, we have:

$$T_2 = T_{02} - \frac{C_2^2}{2c_p} \tag{3.26}$$

$$\frac{P_2}{P_{02}} = \left(\frac{T_2}{T_{02}}\right)^{\frac{\gamma}{\gamma-1}} \tag{3.27}$$

$$\frac{P_2}{P_{01}} = \frac{P_2}{P_{02}} \cdot \frac{P_{02}}{P_{01}} \tag{3.28}$$

$$P_2 = \frac{P_2}{P_{01}} \times P_{01} \tag{3.29}$$

$$\rho_2 = \frac{P_2}{RT_2} \tag{3.30}$$

Diffuser inlet angle

Area of the cross-section of flow in radial direction;

$$A_2 = 2\pi r_2 \times h_2 \tag{3.43}$$

$$C_{r2} = \frac{\dot{m}}{\rho_2 A_2} \tag{3.41}$$

Taking the recent C_{r2}, the angle of the diffuser vane leading edge for zero incidence will be;

$$\theta = \tan^{-1}\left({C_{r2}}/{C_{w2}}\right) \tag{3.44}$$

Static density at diffuser throat

The throat width of the diffuser channel may be found by a similar calculation for the flow at the assumed throat radius.

$$C_{w2} = C_{w2_i} \times \frac{D/2}{r_t} \tag{3.45}$$

Equations (3.41) and (3.42) are applied then, equations (3.26) to (3.30) are reapplied.

Diffuser angle at throat

Area of flow in the radial direction is:

$$A_{r2} = 2\pi r_t \times h_2 \tag{3.46}$$

$$C_{r2} = \frac{\dot{m}}{\rho_2 A_{r2}} \tag{3.47}$$

Direction of flow is still expressed as:

$$\theta = \tan^{-1}\left({C_{r2}}/{C_{w2}}\right) \tag{3.44}$$

Diffuser throat width

$$\dot{m} = \rho_2 A_{r2} C_{r2} = \rho_2 A_2 C_2 \tag{3.48}$$

$$A_2 = A_{r2} C_{r2} / C_2 \tag{3.49}$$

$$A_2 = A_{r2} \sin\theta \tag{3.50}$$

Therefore, the width of the throat in each passage is:

$$b_2 = \frac{A_2}{Z_d \times h_2} \tag{3.51}$$

Inducer relative Mach number on ground

Considering the inlet Mach number at the tip radius of impeller eye,

Inlet velocity = C_{a1} (axial)

Eye tip speed = U_t

Relative velocity at tip is:

$$V_t = \sqrt{C_{a1}^2 + U_t^2} \tag{3.52}$$

Velocity of sound is:

$$a = \sqrt{\gamma R T_1} \tag{3.53}$$

Maximum Mach number at inlet is:

$$M = V_t / a \tag{3.54}$$

Diffuser design result

Considering the specifications stated in section 3.3, the table below gives the mean-line diffuser design result.

DIFFUSER DESIGN			
Design Specifications			
S/N	Parametrs	Unit	Value
1	Width of vanelesss space, W_{vl}	m	0.011
2	Throat mean radius, r_t	m	0.091
3	Depth of Diffuser Passage, h_2	m	0.025
4	Number of Diffuser Vanes, Z_d	1	26
Radial Velocity			
	Parameter	Unit	Value
5	r_2	m	0.066
6	C_{w2}	m/s	345.62
7	A_2	m^2	0.013686552
8	ρ_2	Kg/m^3	2.182534
9	C_{r2}	m/s	21.0904322
10	C_2^2/2C_p	K	59.65074166
11	P_{o2}/P_{o1}	1	5.075805678
Static Density at Diffuser Inlet			
	Parameter	Unit	Value
12	T_2	K	431.1305
13	P_2/P_{02}	1	0.635364
14	P_2/P_{01}	1	3.224985
15	P_2	Pa	3.22E+05
16	ρ_2	K/m^3	2.606376
Diffuser Inlet Angle			
	Parameter	Unit	Value
17	A	m^2	0.010369
18	C_{r2}	m/s	23.3122
19	β	deg	3.859062
Static Density at Diffuser Throat			
	Parameter	Unit	Value
20	C_{w2}	m/s	250.6695
21	C_{r2}	m/s	14
22	C_2^2/2C_p	K	31.35879

23	T_2	K	459.4224
24	P_2/P_{02}	1	0.793661
25	P_2/P_{01}	1	4.028468
26	p_2	Pa	4.03E+05
27	ρ_2	K/m^3	3.055243
Diffuser Angle at Throat			
	Parameter	Unit	Value
28	A_{r2}	m^2	0.0142961
29	C_{r2}	m/s	14.42371582
30	Flow direction, θ	deg	3.293455112
Diffuser Throat Width			
31	A_2	m^2	0.00082125
32	b_2	m	0.001263462
33			
Inducer Relative Mach Number			
	Parameter	Unit	Value
34	Inlet Velocity	m/s	85.26629
35	Eye tip speed	m/s	385.8376
36	V_t	m/s	395.1468
37	a	m/s	343.1143
38	Max Mach at Inlet	1	1.151648

TABLE 3.2: MEAN LINE DIFFUSER DESIGN RESULT

3.4.2 2D AND 3D DESIGN WITH CFTURBO

3.4.2.1 IMPELLER DESIGN WITH CFTURBO

To design the impeller on CFturbo, a new compressor project has to be created which will request for the following parameters:

- Flow rate – mass flow rate (0.63Kg/m^3)
- Energy transmission – total pressure ratio (4)
- Revolutions – 80,000rpm
- Gas name – Air
- Gas model – Perfect
- Total inlet pressure – 1bar
- Total inlet temperature - 20℃

The parameters to be used are chosen based on available data and the values were specified as were stated in section 3.3.

Upon specifying the revolutions to be 80,000rpm, the general machine type that suits the design has been highlighted to be radial compressor with low pressure ratio. This is also in compliance with figure 1.3.

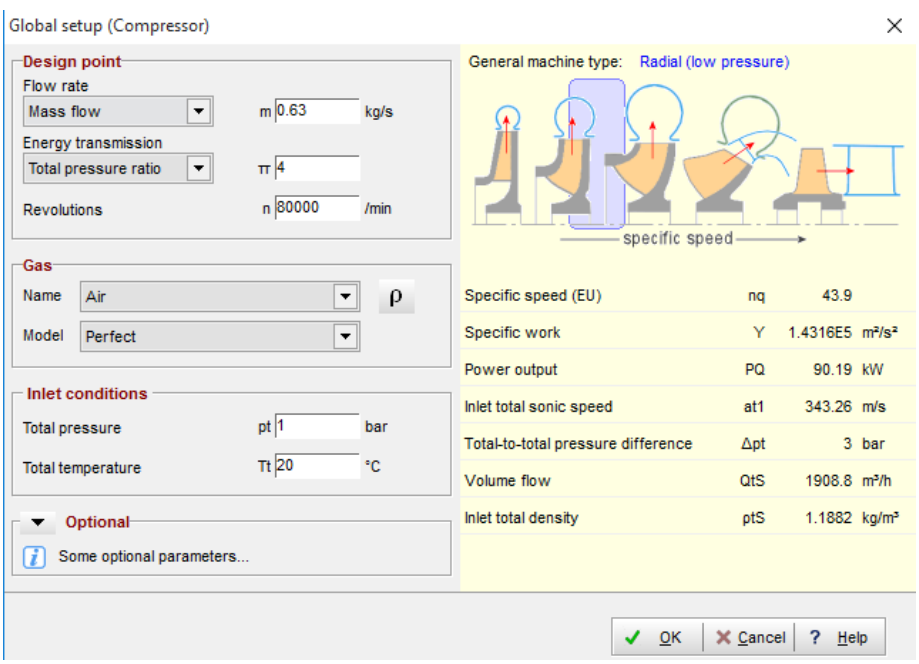

FIGURE 3.8: GLOBAL COMPRESSOR SETUP. ADAPTED FROM CFTURBO

From the impeller main dimension, the diameter was specified (based on specification) as well as outlet width (based on mean line design).

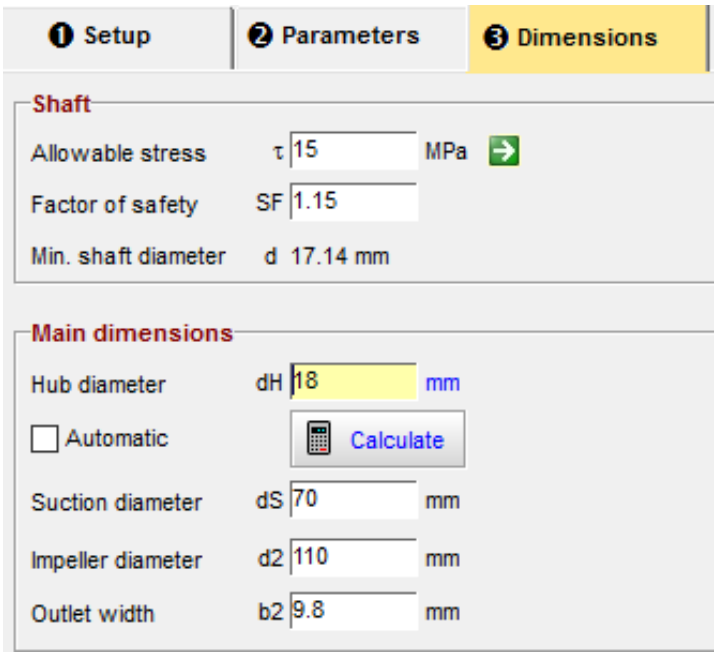

FIGURE 3.9: IMPELLER MAIN DIMENSIONS. ADAPTED FROM CFTURBO

To design an impeller on CFturbo, the following areas will be considered:

- Main dimension – calculate/determine main dimensions
- Meridional contour – design meridional contour
- Blade properties – define blade angles; show velocity triangle
- Blade mean lines – design blade mean lines
- Blade profiles – design blade profiles
- Blade edges – round blade leading/trailing edge
- CFD setup – some additional operations for CFD
- Model settings
- Model finishing

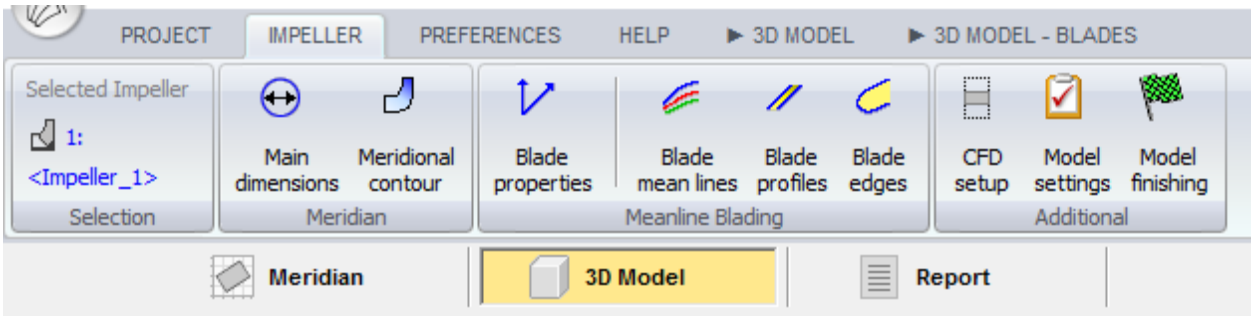

FIGURE 3.10: IMPELLER DESIGN SECTIONS ON CFTURBO

All the sections has inputs by default but can be altered to suit the designer's desire.

From meridional contour of the impeller with the hub and shroud after slight adjustment is as shown below.

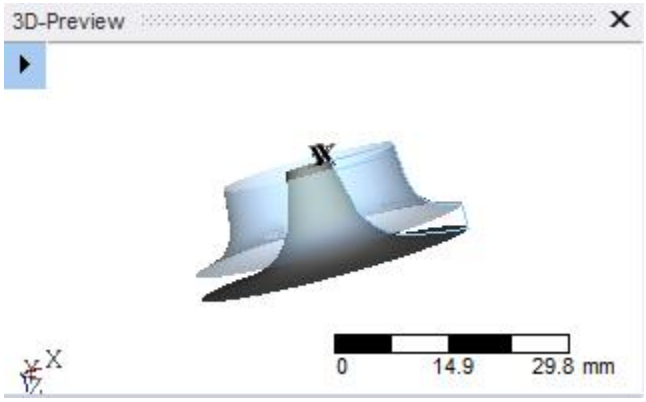

FIGURE 3.11: 3D PREVIEW OF IMPELLER MERIDIONAL PLANE

As calculated during the mean line design, the number of blades is selected to be 20 in the blade properties section.

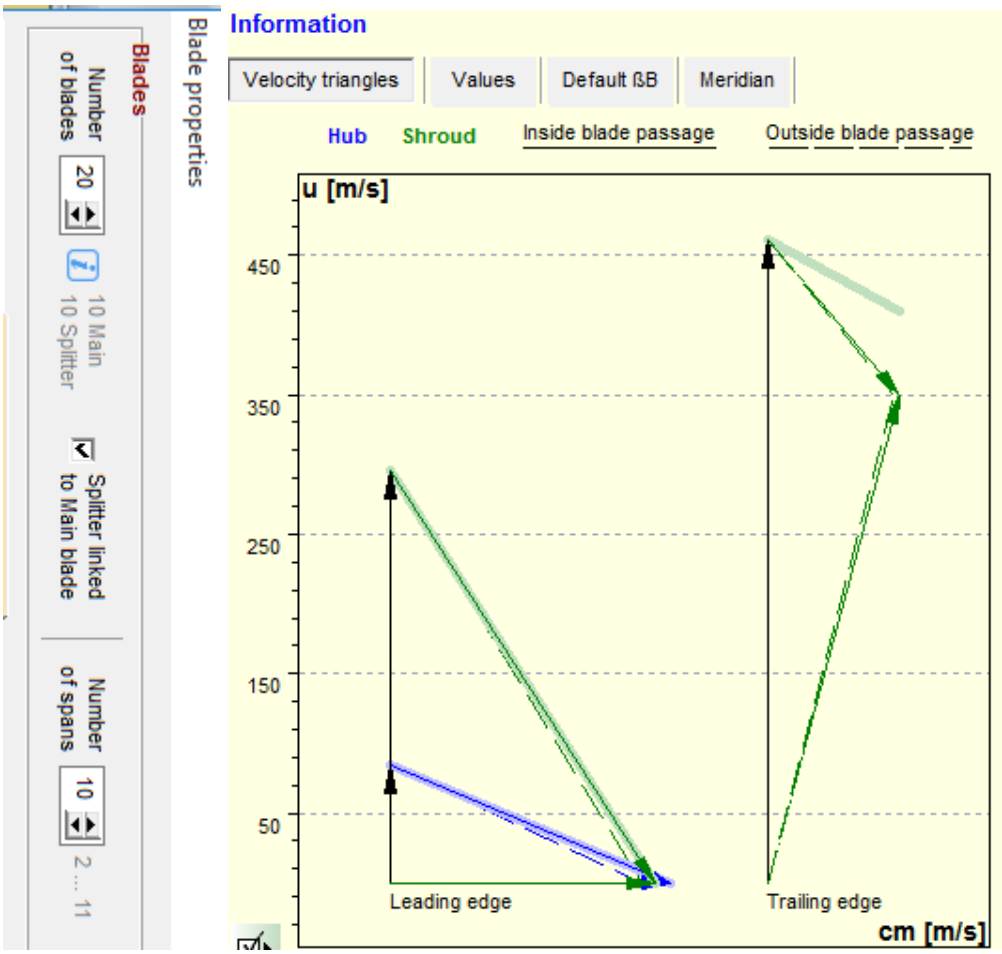

FIGURE 3.12: BLADE PROPERTIES AND VELOCITY TRIANGLE

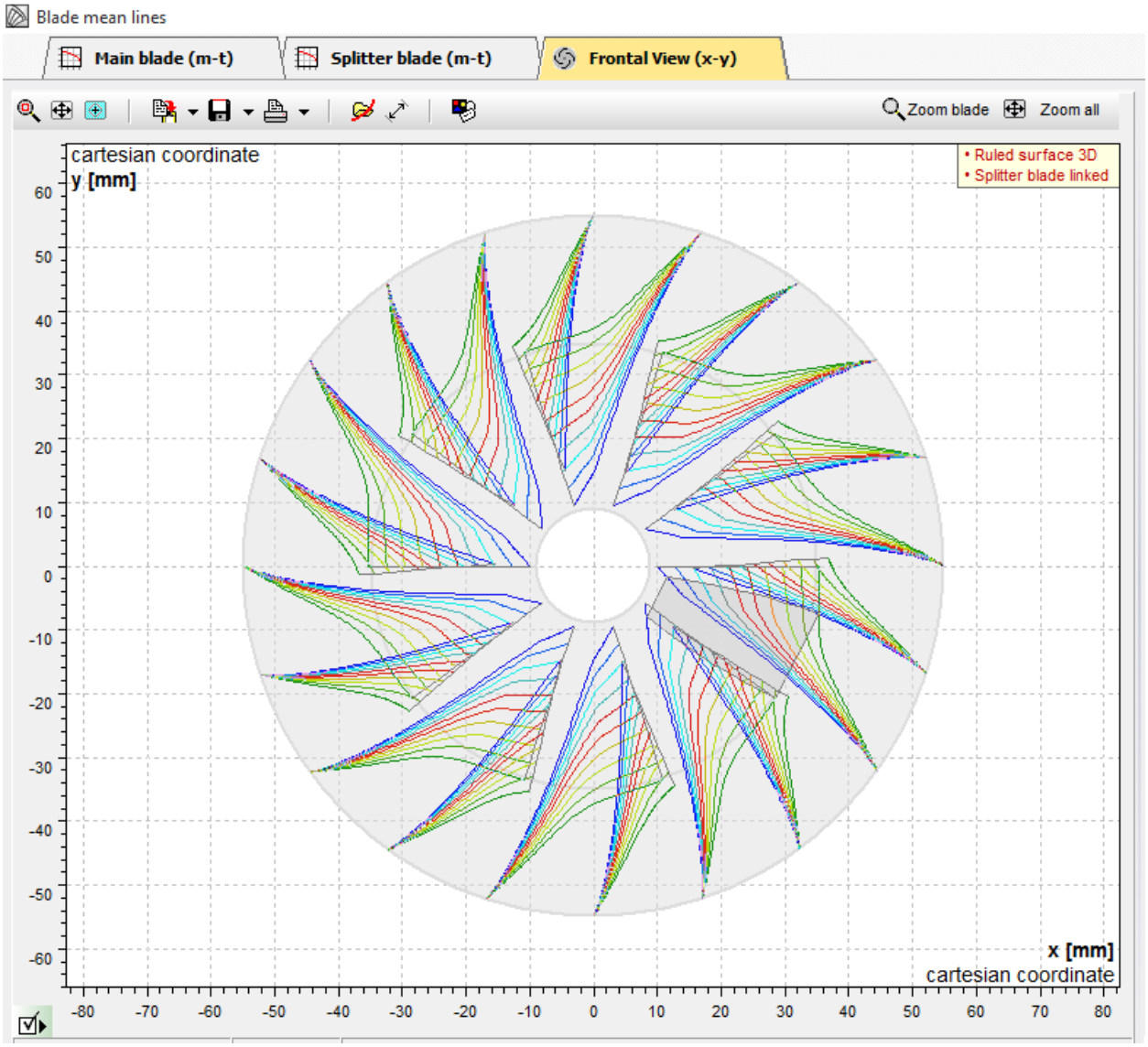

FIGURE3.13: BLADES MEAN LINE FRONT VIEW

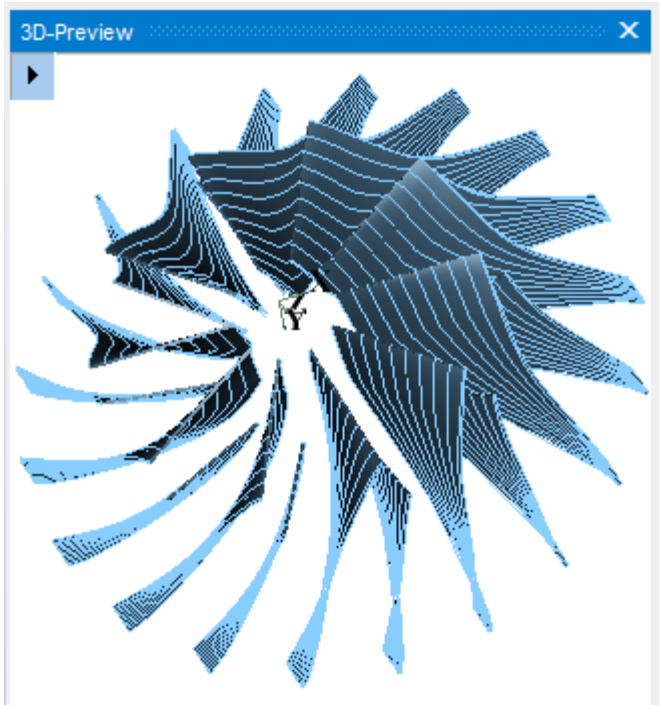

FIGURE 3.14: 3D PREVIEW OF IMPELLER BLADES FROM BLADES PROFILE

Upon completion of the impeller design, the impeller is as shown in the figure below.

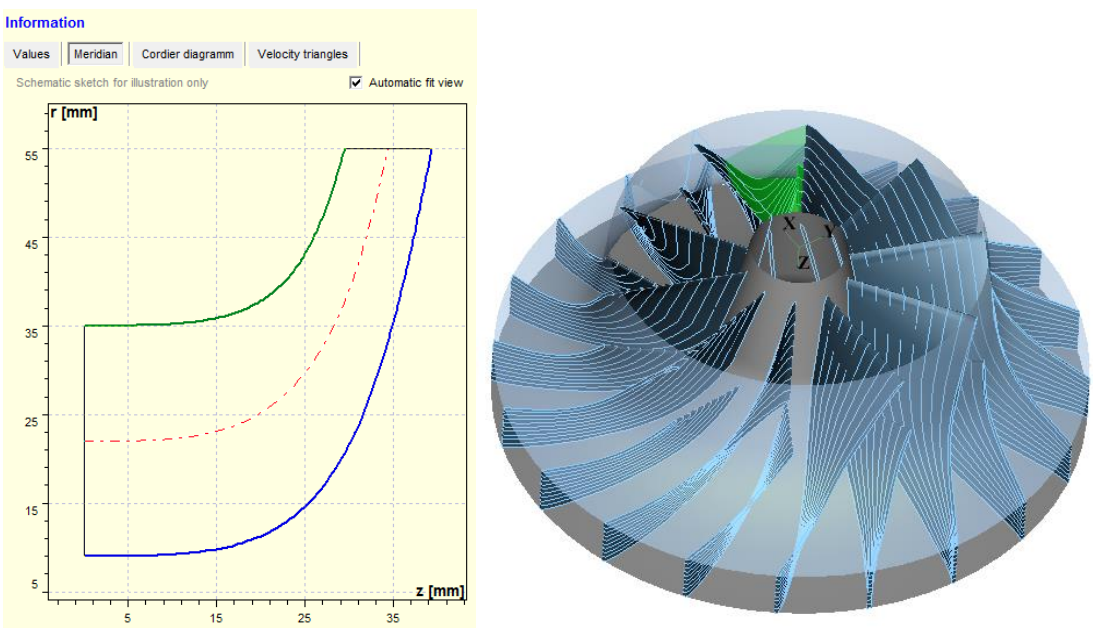

FIGURE 3.15: IMPELLER DESIGN AND MERIDIONAL VIEW. ADAPTED FROM CFTURBO

The design report of the impeller that is prepared by CFturbo is as in the figures below.

Parameter	Symbol	Unit	Value	Value 2
1: <Impeller_1>				
Main dimensions				
Setup				
Unshrouded impeller			Yes	
Tip clearance	x	[mm]	1.267	
Splitter blades			Yes	
Manual dimensioning			No	
Parameters				
Total-to-total efficiency	ηtt	[%]	88.8	
Tip clearance efficiency	ηt	[%]	100	
Mechanical efficiency	ηm	[%]	99	
Motor efficiency	ηmot	[%]	80	
Empirical function for ...			CFturbo d...	
Empirical function for ...			CFturbo d...	
Empirical function for ...			CFturbo d...	
Empirical function for ...			CFturbo d...	
Diameter coefficient	δ	[-]	3.568	
Outlet width ratio	b2/d2	[-]	0.06	
Impeller efficiency	ηIm	[%]	88.8	
Stage efficiency	ηSt	[%]	87.9	
Stage efficiency incl. ...	ηSt*	[%]	70.3	
Empirical function for ...			CFturbo d...	
Meridional deceler.	c2m/cSm	[-]	1	
Required driving power	PD	[kW]	102.6	
Required power incl. ...	PR	[kW]	128.2	

FIGURE 3.16(A): IMPELLER DESIGN REPORT 1. ADAPTED FROM CFTURBO

Parameter	Symbol	Unit	Value	Value 2
Blade properties				
Number of blades	z		20 (10/10)	
Blade shape			Ruled surf...	
Number of meridional sec...			11	
Incidence ratio	RQ	%	100	100
Main blade				
Thickness leading edge	sLE	[mm]	0.6	0.6
Thickness trailing edge	sTE	[mm]	0.6	0.6
Blade angle leading e...	βB1	°	52	14.4
Splitter blade				
Linked to main blade			Yes	
Blade angle trailing edge	βB2	°	70.6	86.2
Automatic calculation			Yes	
Suction side				
Circumferential velocity	u	[m/s]	75.4	385.8
Angle of absolute flow	αF	[°]	90	90
Angle of relative flow	βF	[°]	48.6	12.5
Circumferential comp...	wu	[m/s]	75.4	385.8
Relative velocity	w	[m/s]	114	395.1
Meridional componen...	cm	[m/s]	85.5	85.5
Radial component of ...	cr	[m/s]	10.1	0
Axial component of a...	cax	[m/s]	84.9	85.5
Circumferential comp...	cu	[m/s]	0	0
Absolute velocity	c	[m/s]	85.5	85.5

FIGURE 3.16(B): IMPELLER DESIGN REPORT 2. ADAPTED FROM CFTURBO

Validation of CFturbo design result

To check the validity of CFturbo, its result was compared with that of the mean line design as shown in the table below.

CFTURBO AND MEAN LINE DESIGN RESULTS COMPARISON			
S/N	Parameter	Mean line result	CFturbo result
1	Power required	125.23KW	128.2KW
2	Circumferential velocity at root, U_r	75.41m/s	75.4m/s
3	Circumferential velocity at tip, U_t	385.81m/s	385.8m/s
4	Angle of relative flow at root, β_r	48.5deg	48.6deg
5	Angle of relative flow at tip, β_t	12.46deg	12.5deg
6	Absolute radial velocity at exit, C_{r2}	85.3m/s	85.8m/s

TABLE 3.3: COMPARISON OF CFTURBO DESIGN RESULT AND MEAN LINE DESIGN RESULT

The values stated in the table above are part of the major results of the mean line impeller design. The other parameters have been used as inputs for the main dimensions in the CFturbo design. The results in the table above show good correlation. Hence CFturbo results have been validated.

3.4.2.2 DIFFUSER DESIGN WITH CFTURBO

To design the diffuser, a new component has to be added to the impeller. On the dialogue box that appears, new stator will be selected. The main dimensions are then specified. Here, the stator type was considered to be radial diffuser and the depth of the diffuser passage (25mm) which was specified earlier was used to define the extent (diffuser inlet to outlet) of hub and shroud.

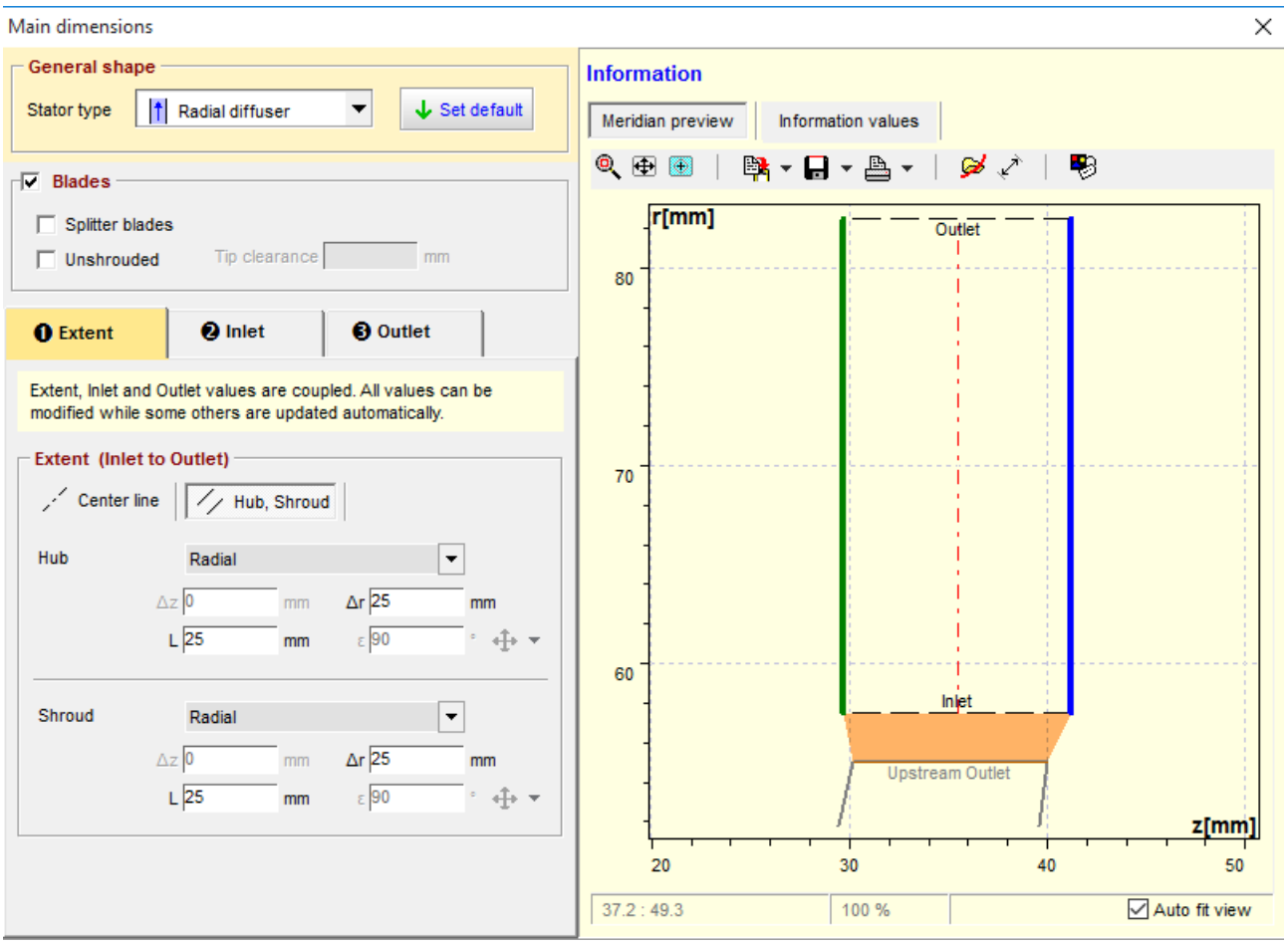

FIGURE 3.17: DIFFUSER DESIGN MAIN DIMENSIONS

Just like impeller design, diffuser design sections are: main dimensions, meridional contour, blade properties, blade mean lines, blade profile, blade edges, CFD setup, model setting, and model

finishing. The steps are sequential. The designer can't jump a step to the next. Each steps has to be reviewed before going to the next, even though there are default inputs on each step.

From the meridional contour, the diffuser appears in form of a rectangle and the 3D preview is as in the figure below.

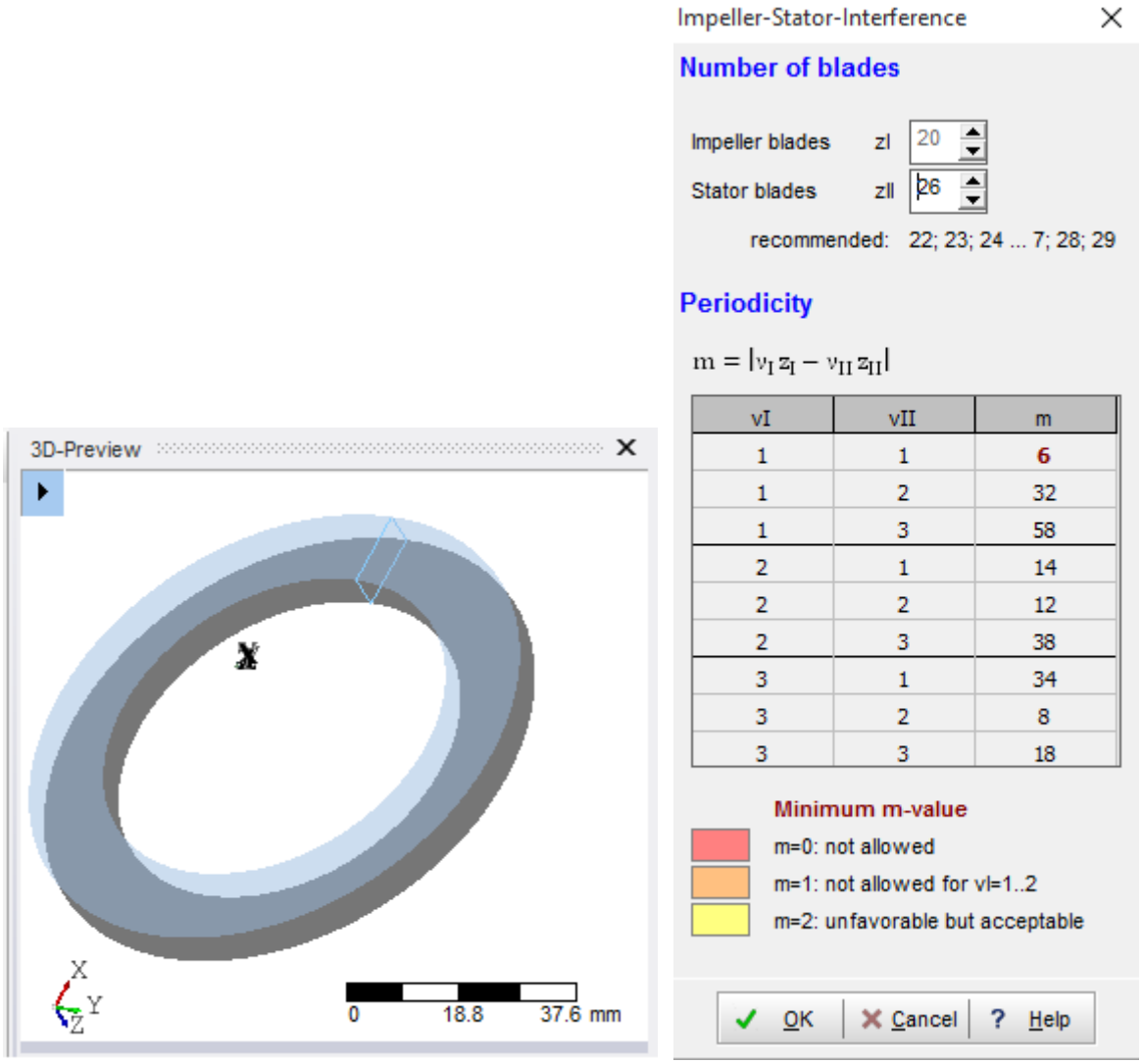

FIGURE 3.18: (A) 3D PREVIEW OF DIFFUSER MERIDIONAL PLANE (B) IMPELLER-STATOR-INTERFERENCE

In the blade properties, the number of blades was selected to be 26 as stated earlier. The periodicity table under the Impeller-stator-interference ribbon was used to check the acceptability of the number of blades. A value of the periodicity that is less than 2 will not be accepted. The selected number (26) is acceptable as shown in the figure above. If not, the cell(s) that is not in compliance with the minimum periodicity value stated will be highlighted with the relative color.

After the blade properties, the front view of the blade mean lines is viewed and is as in the figure below.

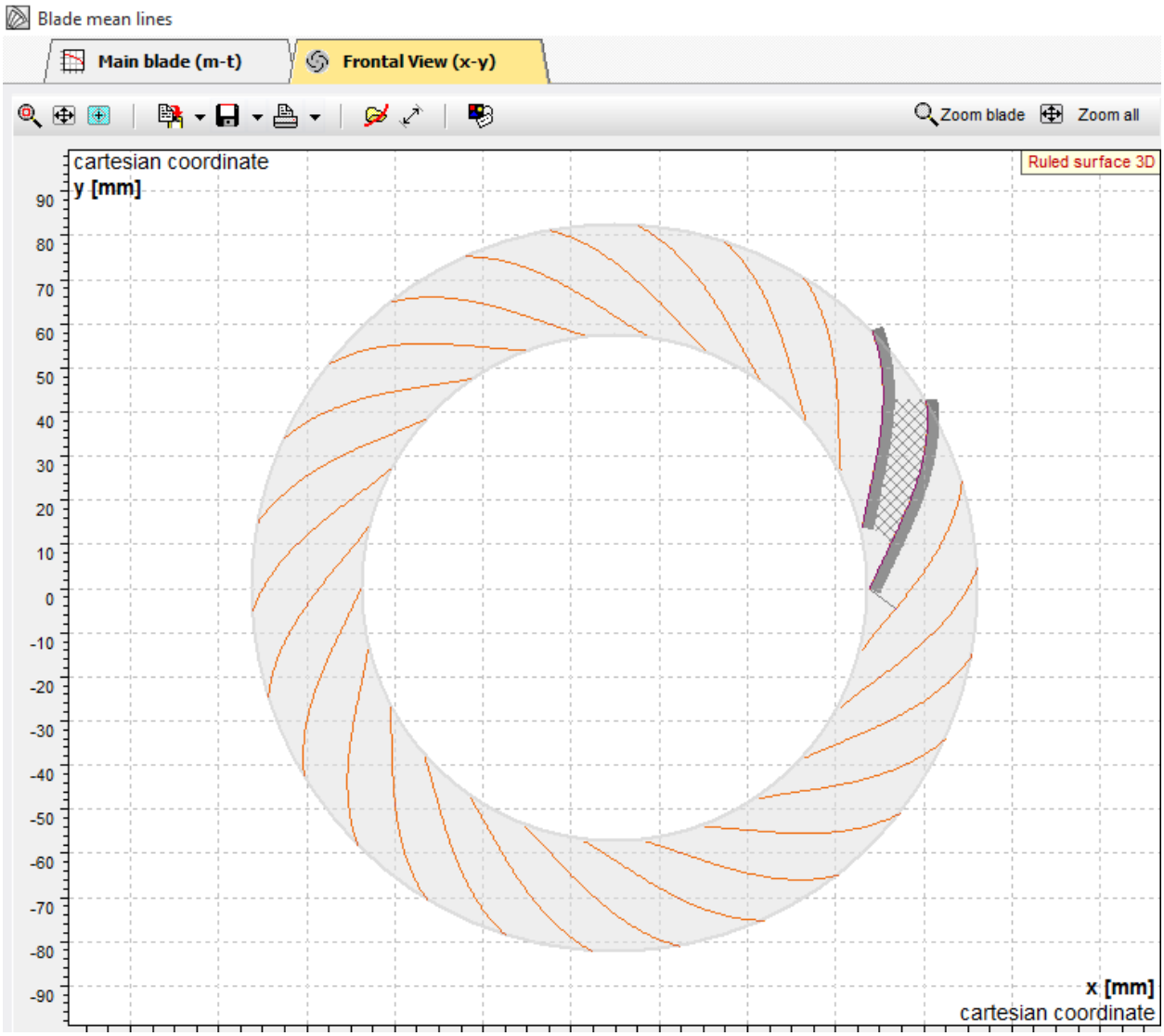

FIGURE 3.19: FRONT VIEW OF DIFFUSER BLADE MEAN LINES

The blade edge is selected to Bezier and was adjusted to ensure streamlined edge.

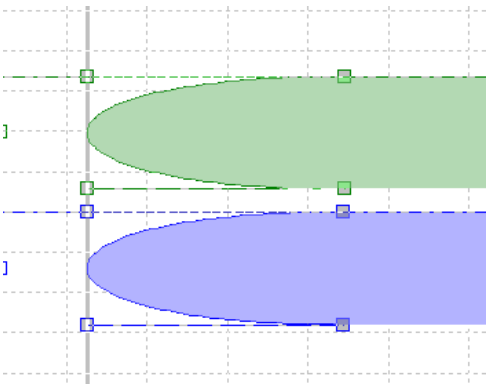

FIGURE 3.20: DIFFUSER BLADE EDGES

After model finishing, the final diffuser design, coupled with the impeller design is as shown in the figure below

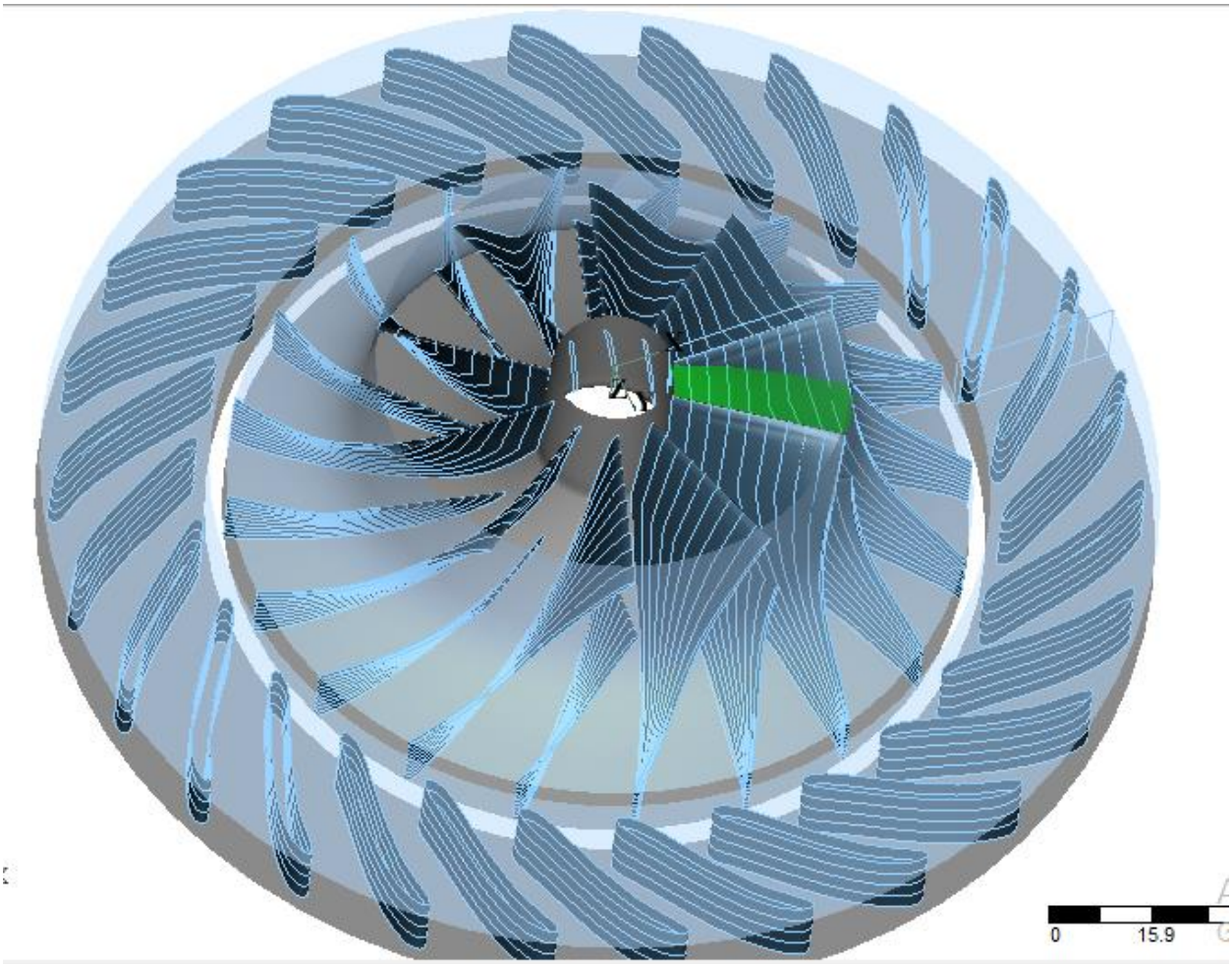

FIGURE 3: 21: COMPRESSOR DESIGN - IMPELLER WITH DIFFUSER

CHAPTER 4

4.1 CFD ANALYSIS

This section covers the application of computational fluid dynamics to check for the performance of the designed compressor on. It covers the generation of geometry (using Ansys BladeGen) and the use of Ansys Turbomachinery to generate the mesh, set up the system, obtain the solution and view the result. Figure 4.1 shows the project schematic on Ansys.

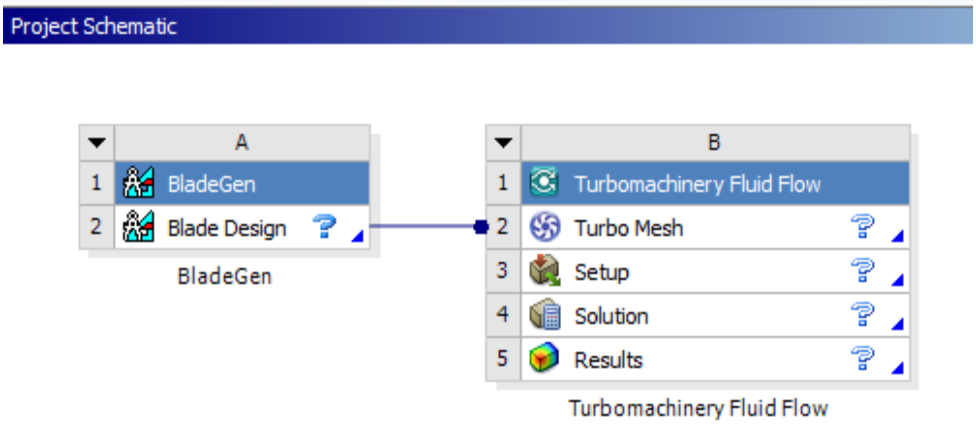

FIGURE 4.1: CFD ANALYSIS SCHEMATIC. ADAPTED FROM ANSYS.

4.2 GENERATION OF GEOMETRY ON ANSYS BLAGEDEN

The first thing to do in the analysis of the compressor is to generate the geometry to be analyzed. There are two approaches to this. The design on the CFturbo can be exported to a format compatible with Ansys and then imported or the same compressor can be designed on Ansys using BladeGen. The second approach appear to be more convenient to work with as it is easier to change the blade angle which makes comparison of impellers with different blade angles easy. Also, Turbogrid (turbo mesh tool) automatically determines the inlet, outlet and fluid domain.

To create the geometry, Blade design was loaded and initial Meridional Configuration Dialog which requires the coordinates of the impeller inlet and outlet comes up. Also, the machine type has to be specified. Here, the coordinates were copied from CFturbo and were used to primarily define the impeller. For the upper and lower parts of the meridional configuration, i.e. shroud and hub respectively, ten(10) points are considered for each in ordered to obtain a geometry very close to that of the CFturbo design. The blade angle was changed to 12deg and the number

of blades was specified to be 20. A sectional view of the 3D blade showing two blades is as depicted in figure 4.3.

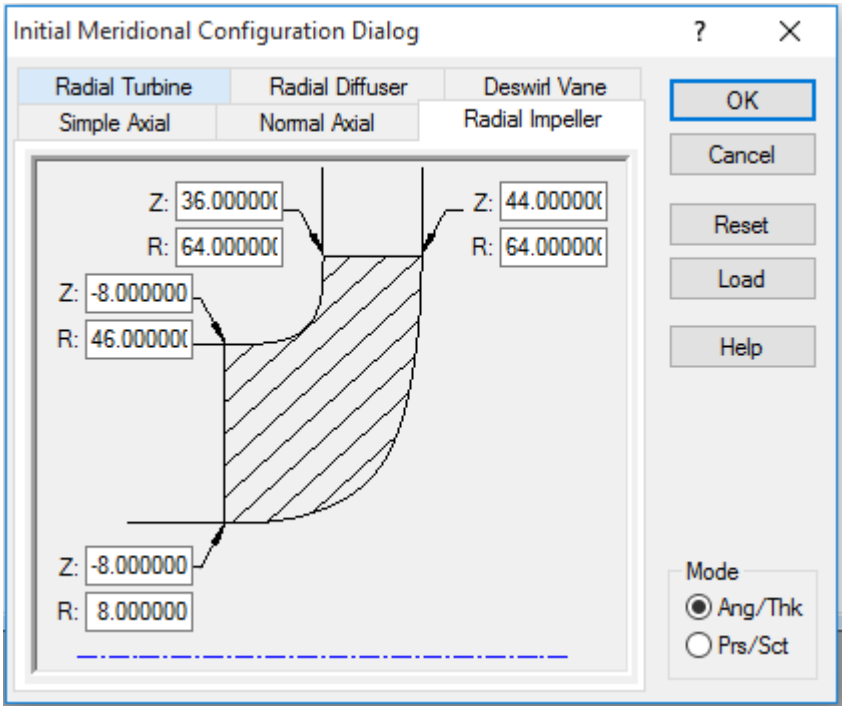

FIGURE 4.2: IMPELLER MERIDIONAL CONFIGURATION DIALOG FOR IMPELLER GEOMETRY. ADAPTED FROM ANSYS BLADEGEN

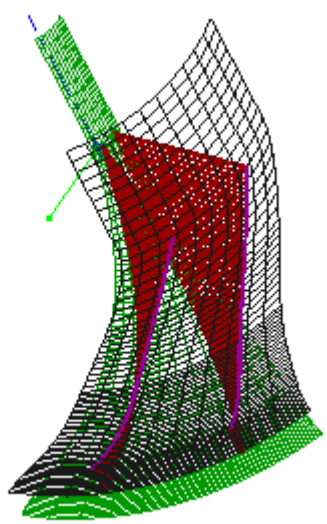

FIGURE 4.3: SECTIONAL VIEW OF 3D IMPELLER

4.3 MESH GENERATION

In Ansys Turbomachinery Fluid Flow, Mesh is generated through the use of TurboGrid. As stated earlier, inlet and outlet is identified by default. The following are specified for mesh generation.

- Geometry > Machine data > activate rotation and select the following
    - Method – Principal Axis
    - Axis – Z
    - Base Units – mm
    - Machine type – Centrifugal compressor
    - Select Apply
- Mesh Data > Mesh Size
    - Method – Target Passage Mesh Size
    - Node Count – Fine (250000)
    - Boundary Layer Refinement Control > Method – Proportional to Mesh Size
    - Select Apply
- Mesh Data > Derails of Mesh Data > Passage
    - Method – Element Count and Size
    - # of Elements – 50
    - Select Apply
- Mesh Data > Inlet/Outlet
    - Inlet Domain
        - Mesh Type – H-Grid
        - Activate override default # of Elements
        - # of Elements – 50
    - Outlet Domain
        - Mesh Type – H-Grid
        - Activate override default # of Elements
        - # of Elements – 50
        - Select Apply
- 3D Mesh > Click on Generate

After clicking on Generate, a fine mesh appeared on the impeller section being operated with as in figure 4.4 below

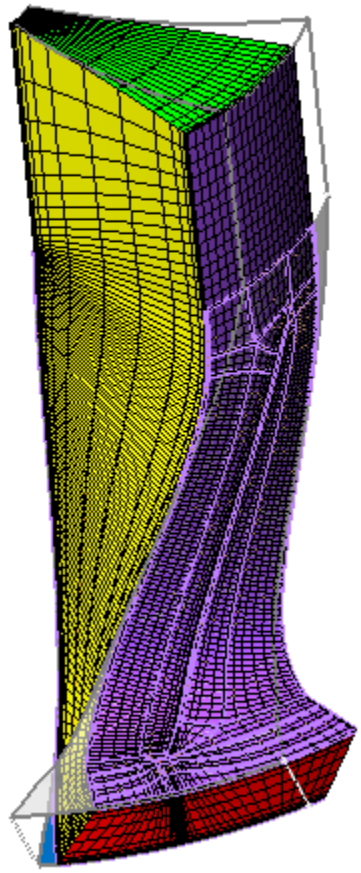

FIGURE 4.4: IMPELLER MESH. ADAPTED FROM ANSYS TUBOGRID

4.4 CFD SETUP

In turbomachinery fluid flow, CFX is used for setup. This identifies the inlet, outlet and flow domain by default.

In setting up the analysis, the following were considered.

- Simulation > Flow Analysis 1 > Default Domain > Basic Settings
    - Domain Type – Fluid Domain
    - Fluid 1
        - Option – Material Library
        - Material – Air at 25 C

    - Morphology Option – Continuous Fluid
    - Domain Models Reference Pressure – 1atm
    - Buoyancy Model Option – Non Buoyant
    - Domain Motion option – Rotating
    - Domain Motion Angular Velocity – 80000rpm
    - Axis Definition Option – Coordinate Axis
    - Axis Definition Rotation Axis – Global Z
    - Mesh Deformation Option – None
- Simulation > Flow Analysis 1 > Default Domain > Fluid Models
    - Heat transfer Option – Thermal Energy
    - Turbulence Option – K-Epsilon
    - Turbulence Wall Function – Scalable
    - Combustion Option – None
    - Thermal Radiation Option – None
- Simulation > Flow Analysis 1 > Default Domain
    - Default Domain Default
        - Basic settings
            - Boundary type – Wall
            - Frame type – Rotating
        - Boundary Details
            - Mass and Momentum Option – No Slip Wall
            - Wall Roughness Option – Smooth Wall
            - Heat Transfer Option – Adiabatic
    - Inlet
        - Basic Settings
            - Boundary Type – Inlet
            - Location – INBlock INFLOW
            - Frame Type – Rotating
        - Boundary Details
            - Flow Regime Option – Subsonic
            - Mass and Momentum Option – Static Pressure

        - Mass and Momentum Relative Pressure – 101.5KPa
        - Flow Direction Option – Normal to Boundary Condition
        - Turbulence option – Medium (Intensity = 5%)
        - Heat Transfer Option – Static Temperature (20C)
    - Outlet
        - Basic Settings
            - Boundary Type – Outlet
            - Location – Passage OUTFLOW
            - Frame Type – Rotating
        - Boundary Details
            - Option – Subsonic
            - Mass and Momentum Option – Static Pressure
            - Mass and Momentum Relative Pressure – 410KPa

4.5 SOLUTION AND RESULT

The solution for the analysis is conducted by CFX Solver. The solution is obtained by applying the conditions specified in setup to the governing equations. This final result is obtained after several iterations has been performed and the solution has converged.

The result of this analysis is as shown in the figure below. Inlet pressure was specified to be 101.5Kpa and the maximum pressure produced based on this analysis is 410KPan which confirms the pressure ratio of 4.

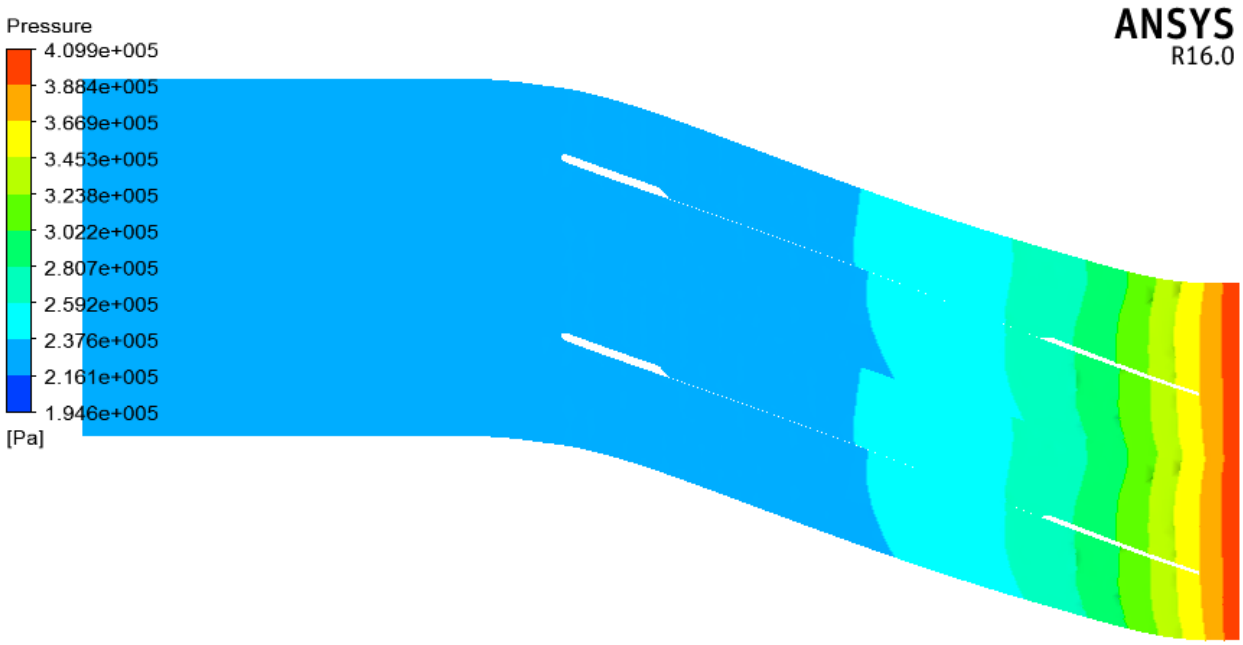

FIGURE 4.5.1: STATIC PRESSURE (BLADE TO BLADE)

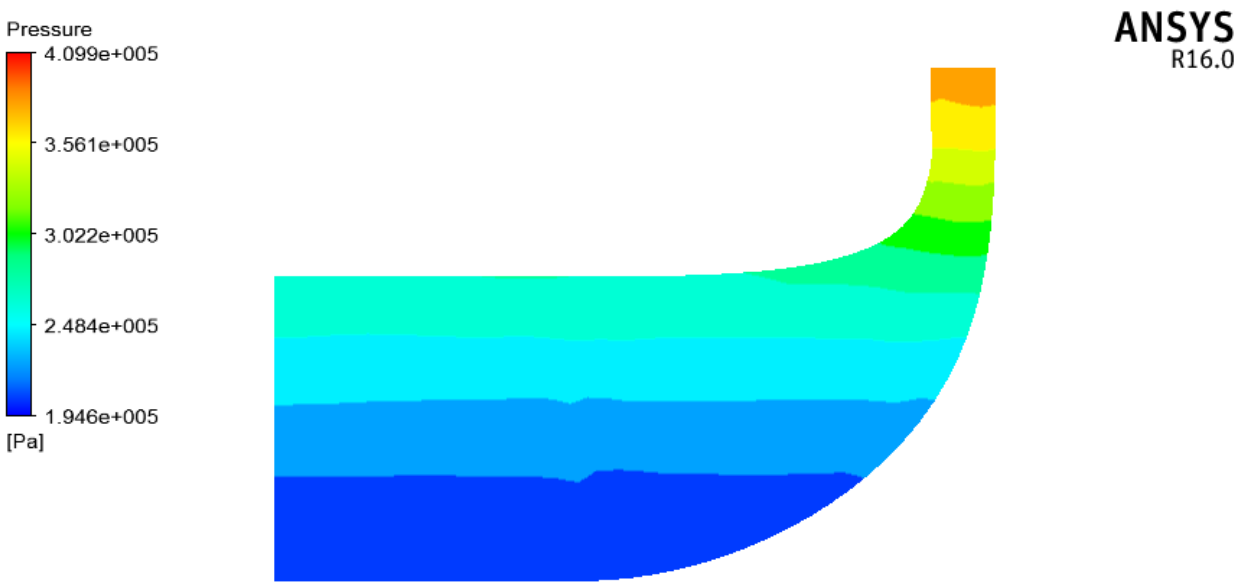

FIGURE 4.5.2: STATIC PRESSURE (MERIDIONAL)

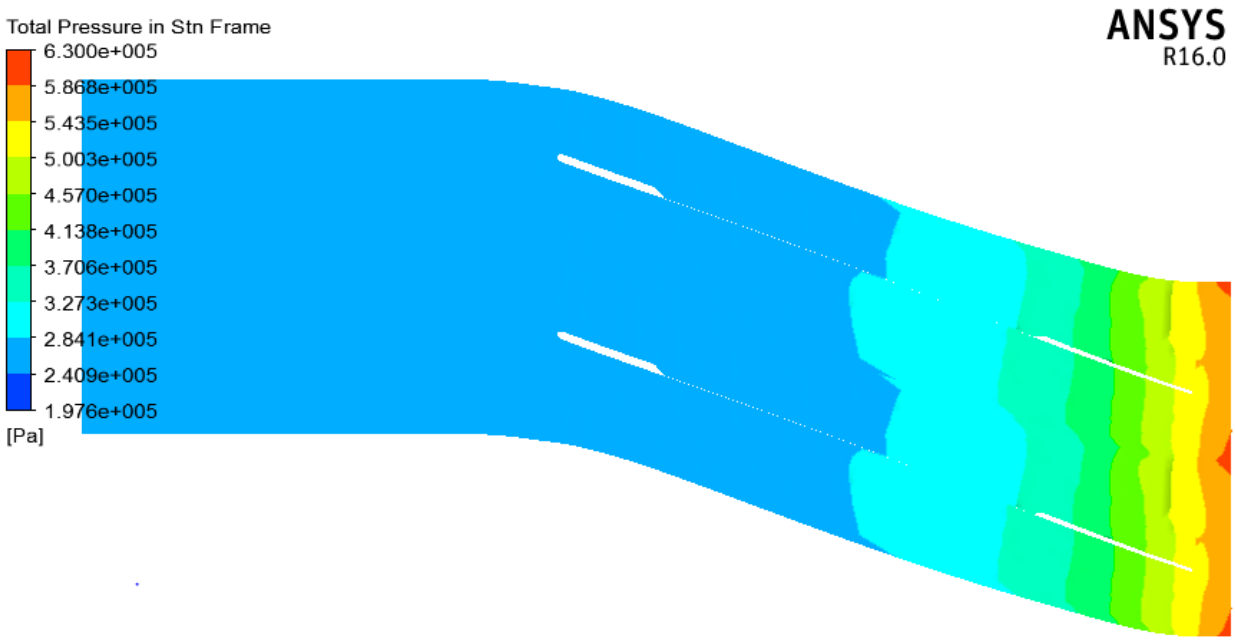

FIGURE 4.6.1: TOTAL PRESSURE (BLADE TO BLADE)

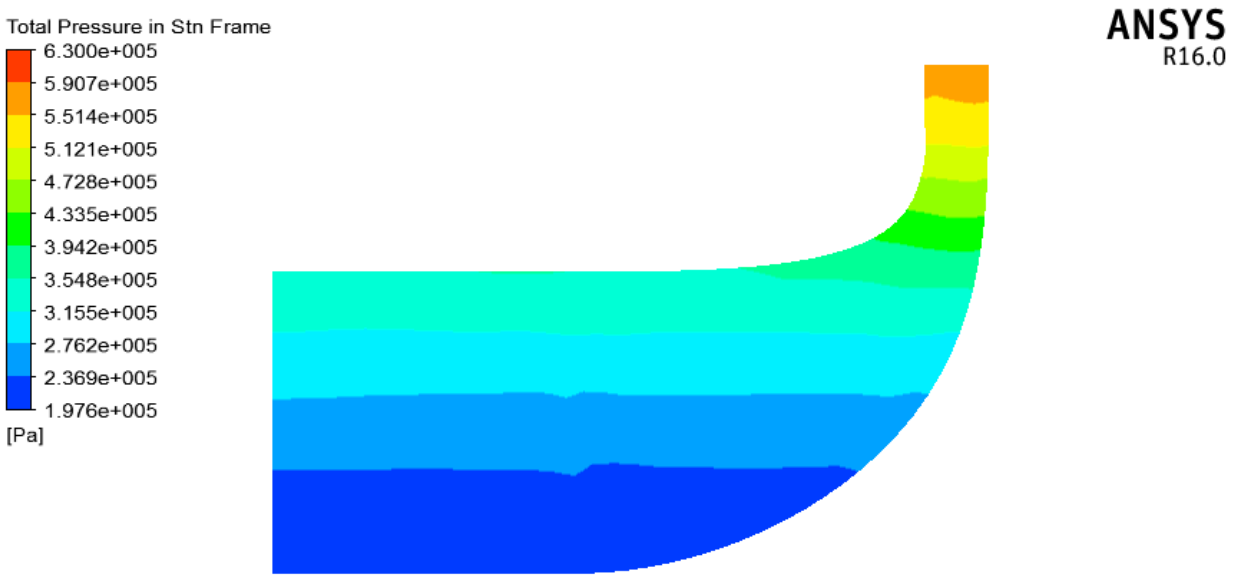

FIGURE 4.6.2: TOTAL PRESSURE (MERIDIONAL)

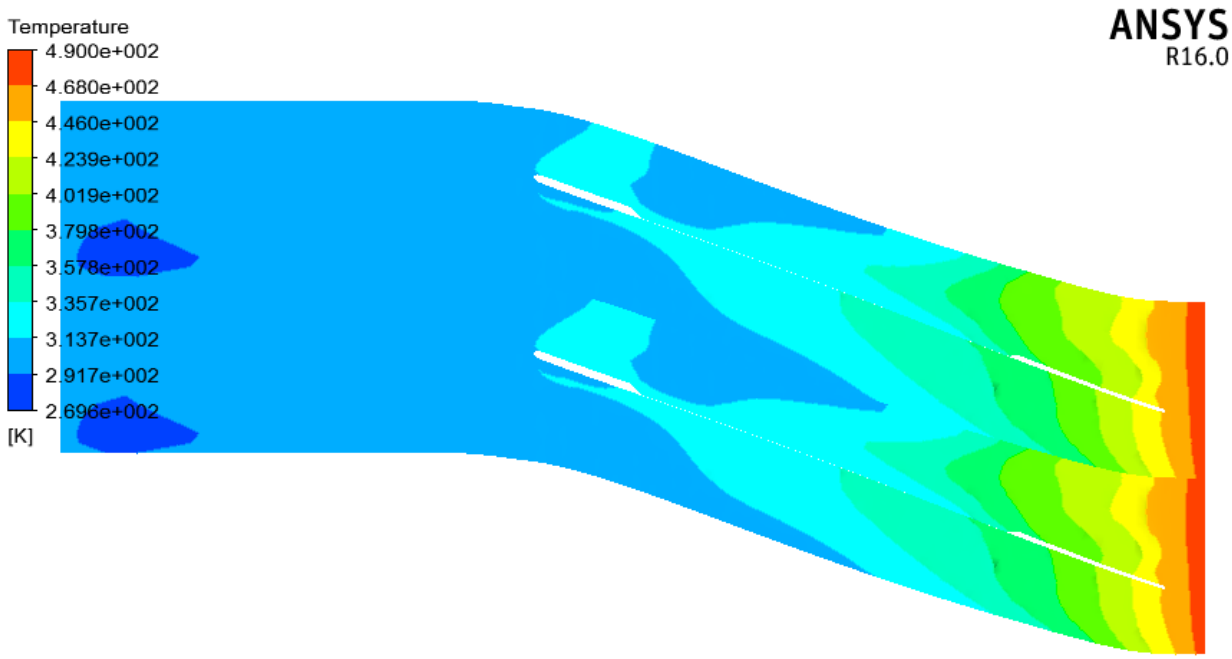

FIGURE 4.7.1: STATIC TEMPERATURE (BLADE TO BLADE)

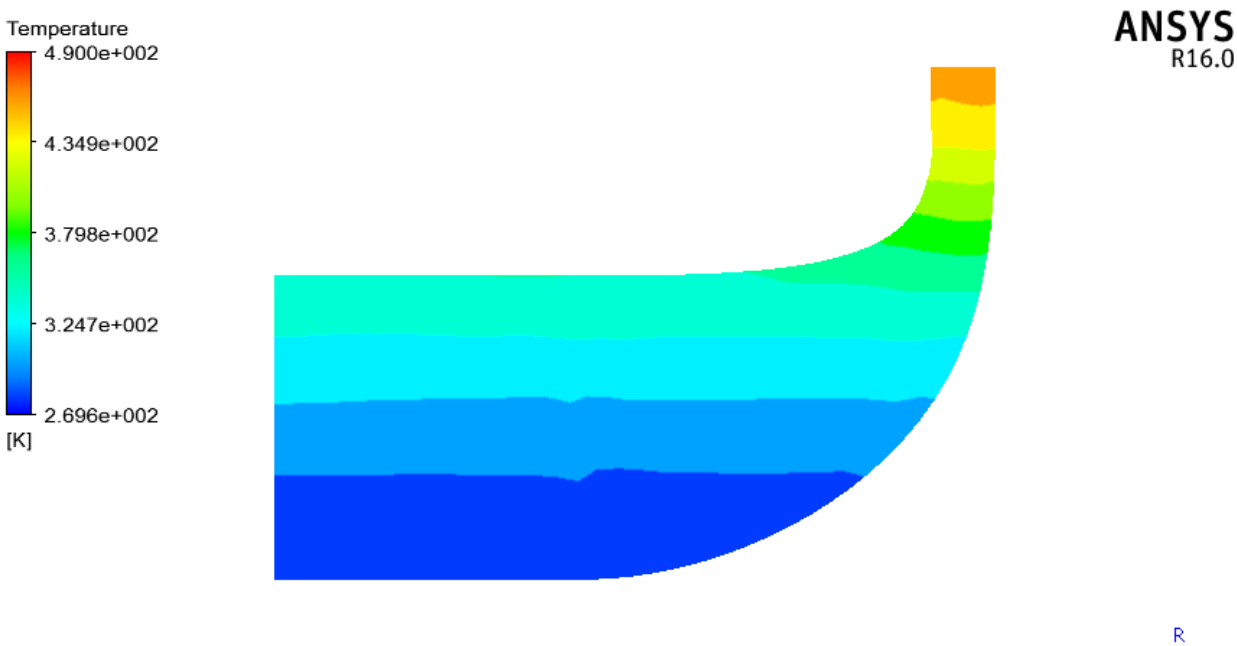

FIGURE 4.7.2: STATIC TEMPERATURE (MERIDIONAL)

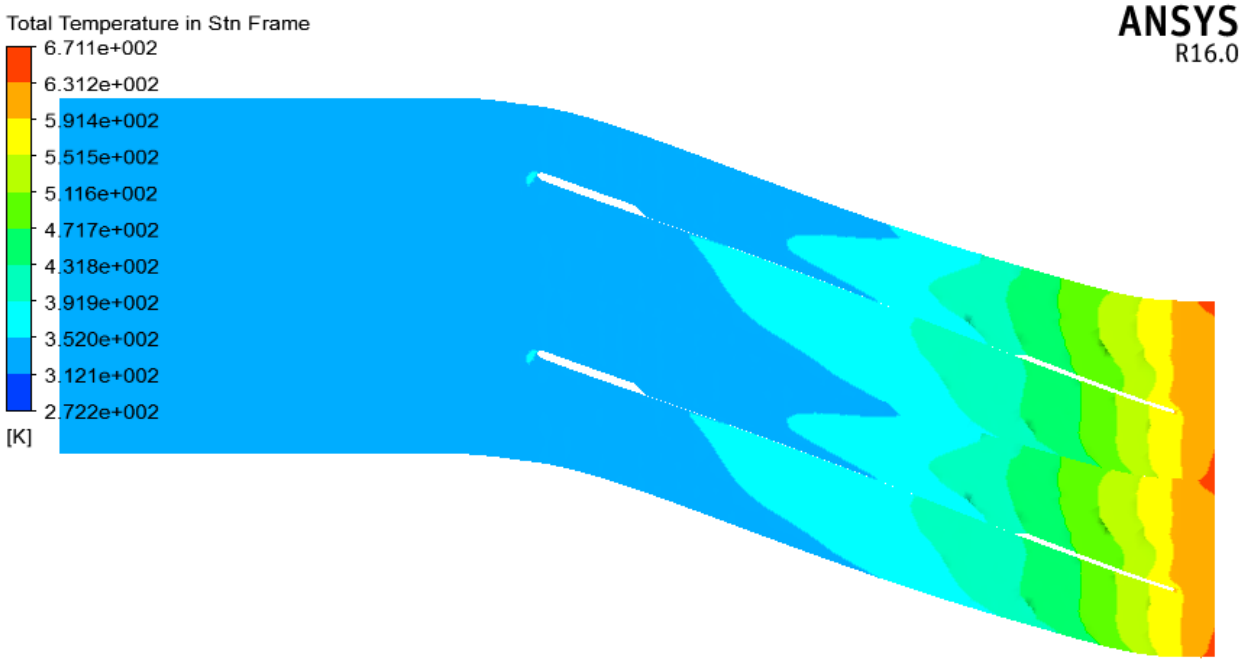

FIGURE 4.8.1: TOTAL TEMPERATURE (BLADE TO BLADE)

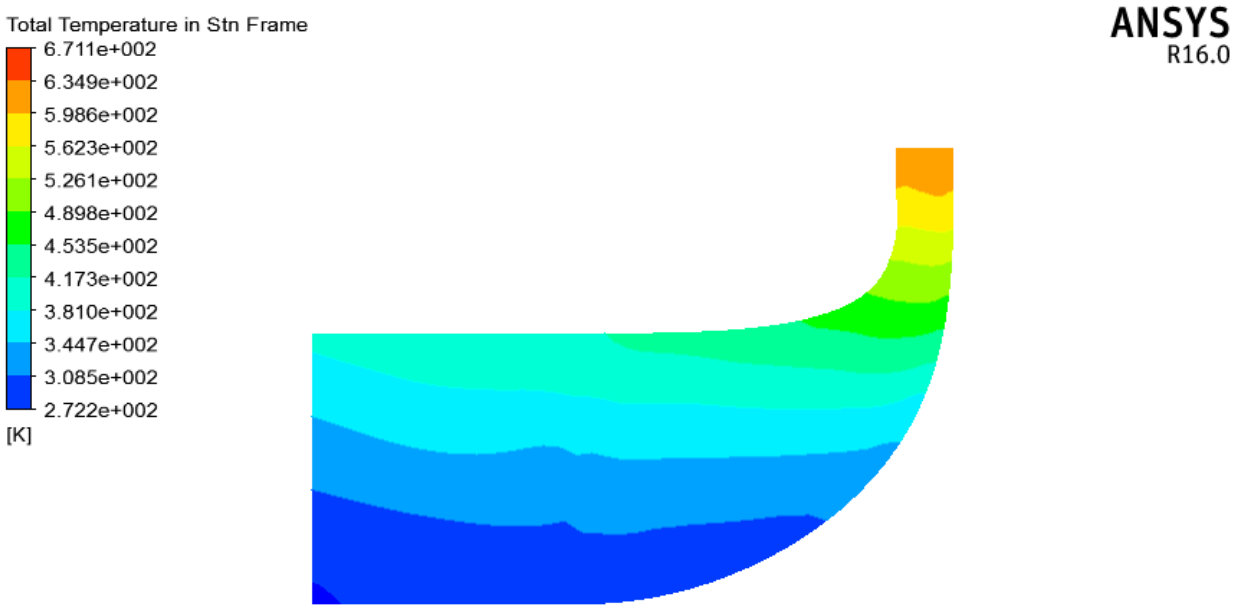

FIGURE 4.8.2: TOTAL TEMPERATURE (MERIDIONAL)

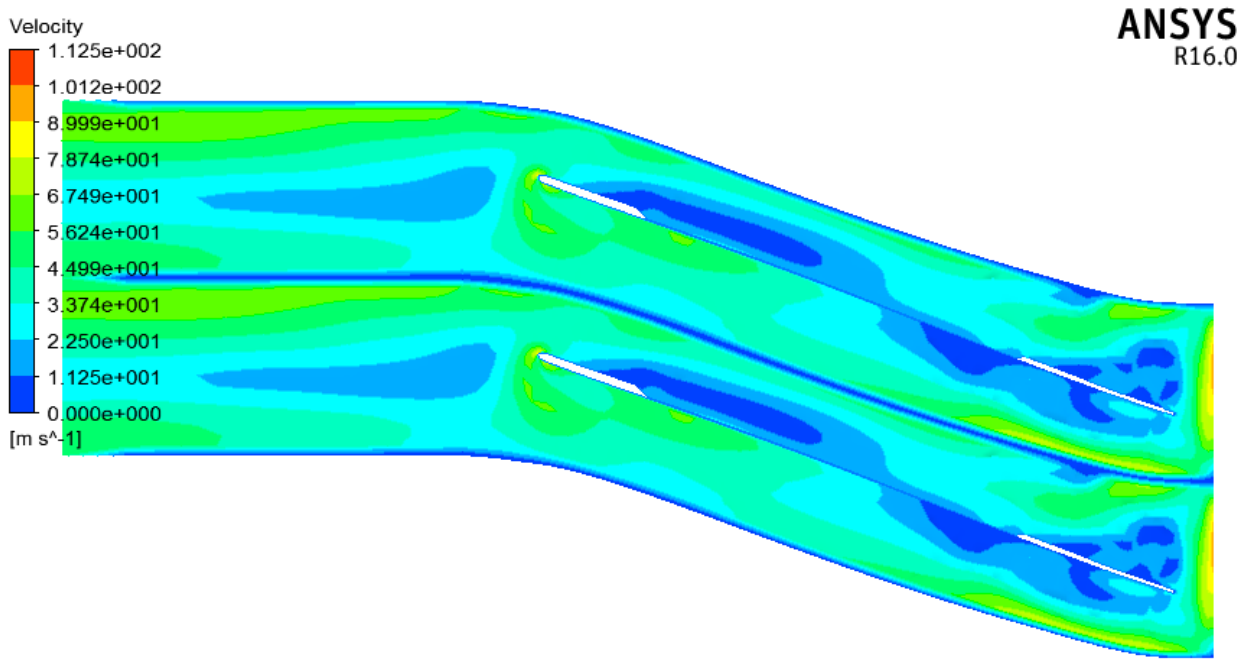

FIGURE 4.9.1: VELOCITY CONTOUR (BLADE TO BLADE)

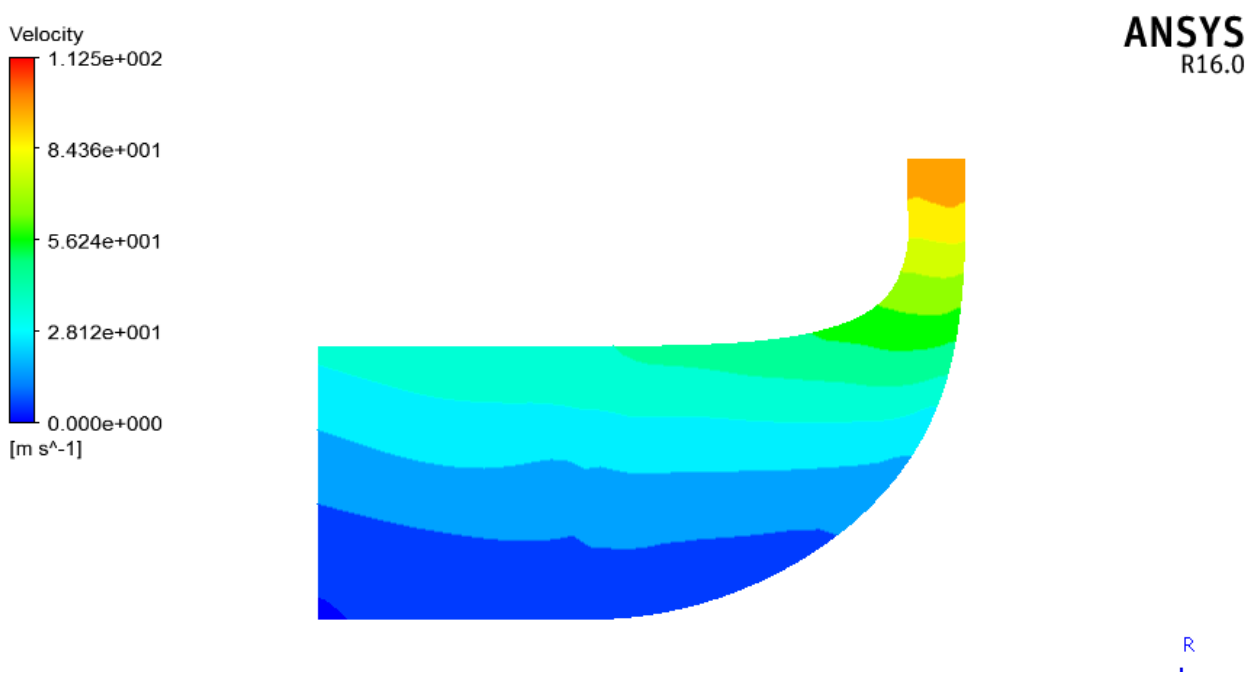

FIGURE 4.9.2: VELOCITY CONTOUR (MERIDIONAL)

4.6 FINAL DESIGN DRAWING

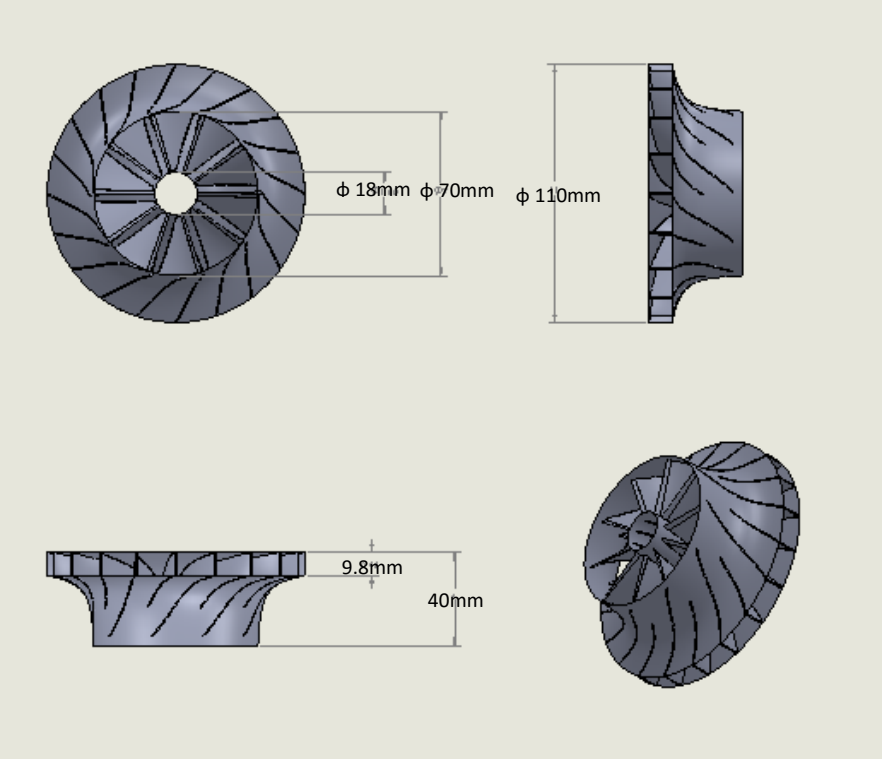

FIGURE 4.10.1: IMPELLER DIAGRAM AND DIMENSION. ADAPTED FROM SOLIDWORKS DRAWING

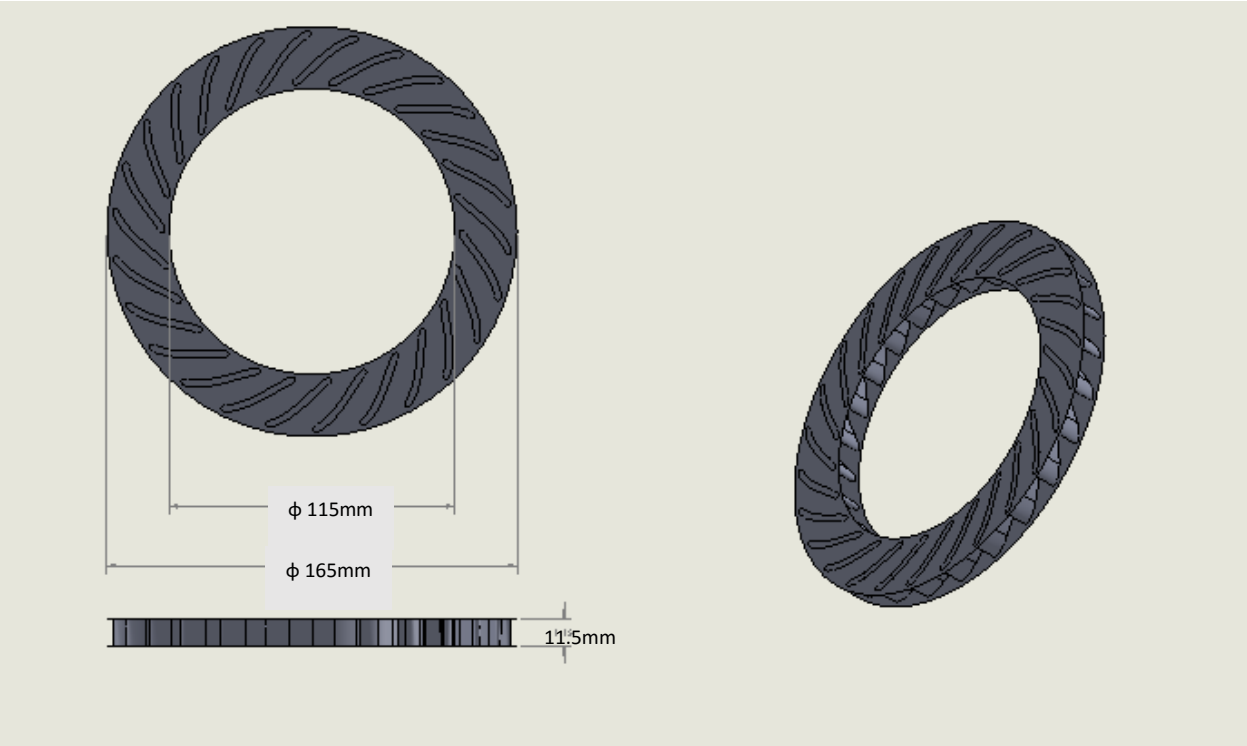

FIGURE 4.10.2: DIFFUSER DIAGRAM WITH DIMENSIONS. ADAPTED FROM SOLIDWORKS DRAWING

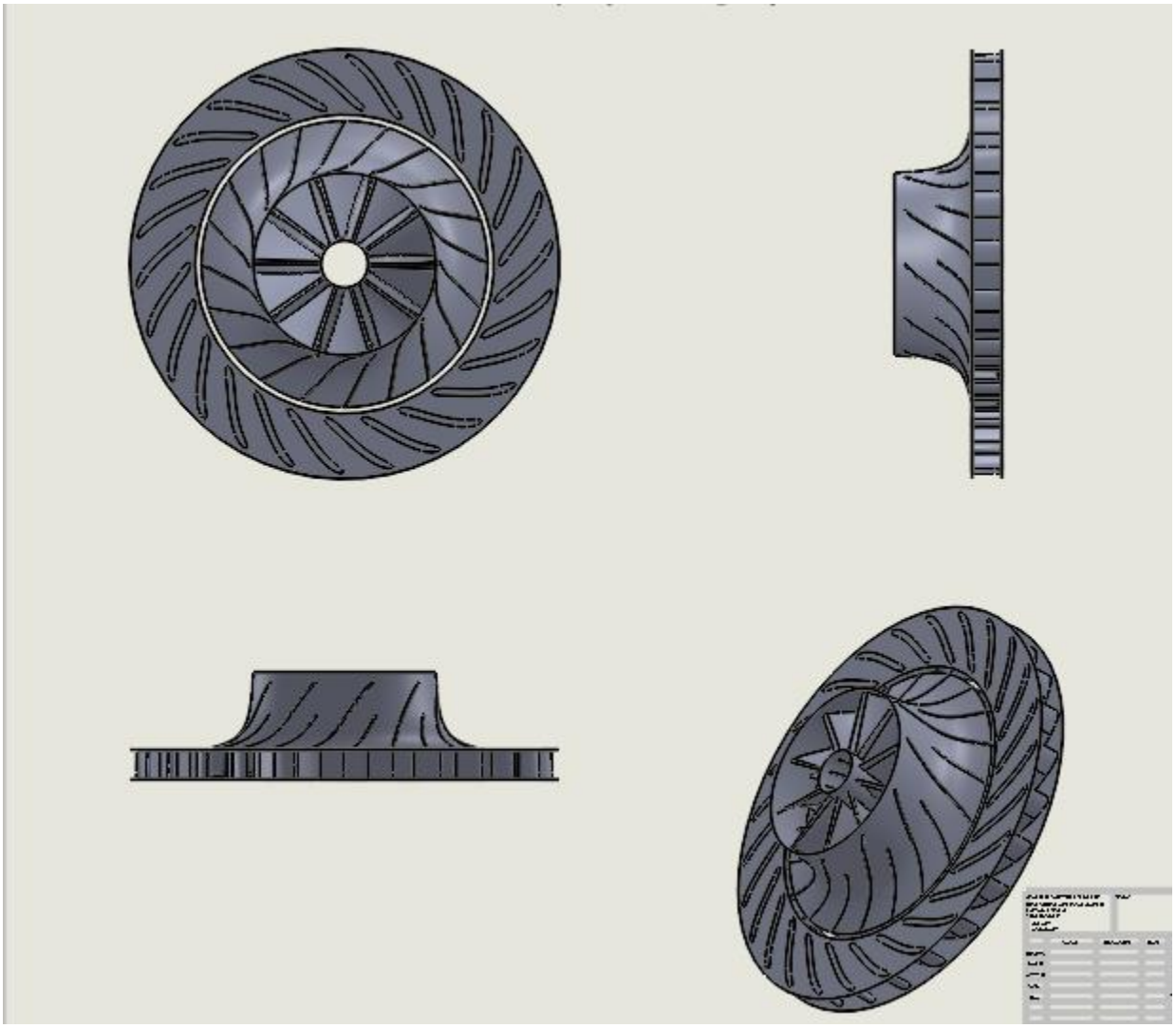

FIGURE 4.10.3: DESIGNED CENTRIFUGAL COMPRESSOR (IMPELLER AND DIFFUSER) DIAGRAM. ADAPTED FROM SOLIDWORKS DRAWING.

CHAPTER 5

5.1 CONCLUSION

CFturbo design result is valid as the validity check done by comparing the results obtained with that of the mean line design (use of equation) showed good correlation. CFD analysis also depict consistency with the aforementioned. Hence, subsequent designs for centrifugal compressors can be done directly using CFturbo. The designed compressor with 20 impeller blades and 26 diffuser vanes, 12.5deg blade, impeller diameter of 110mm, etc. satisfies the pressure ratio requirement of 4. Since the designed impeller blade angle is less 90deg, the blade is backward swept.

5.2 RECOMMENDATION

A centrifugal compressor has been designed which satisfies the stated design requirements. However, not all possible areas are covered in this work. This section covers the recommendations of such areas for further research. The areas are:

1. Experimental analysis of the designed compressor performed through the design and construction of a Test Bed. Here, the designed compressor has to be constructed (or 3D printed).
2. CFD analysis of diffuser contributions to compressor performance
3. A study on the effect of shroud on centrifugal compressors.
4. The effect of splitter blades and its contribution to the blade efficiency
5. Study of the effect of shock wave on compressor performance

5.3 REFERENCES

1. Aghaei. A., and Tousi, A. M. (January 2007). Design and CFD Analysis of Centrifugal Compressor for a Micro Gas Turbine. Niroo Research Institute of Iran, Tehran, Iran.
2. Albaali, G., and Farid, M. M. (February 2006). Fundamentals of Computational Fluid Dynamics.
3. Anand, V. (April 2007). Design Methodology for Aerodynamic Design of Centrifugal Compressor. BTech Thesis, VIT University, Tamil Nadu, India: School of Mechanical and Building Sciences.
4. Andrei, I. C., Niculescu, M. L., Pricop, M. V., and Cernat, A. (2016). Study of the Turbojet Engines as Propulsion Systems for the Unmanned Aerial Vehicles. National Institute for Aerospace Research.
5. Author and Date Not Available. Centrifugal Fan Design Methodologies. Studies on Radial Tipped Centrifugal Fan.
6. Author and Date Not Available. Compressor: Chapter 7. Process Technology Equipment.
7. Bhardwaj, S., Gupta, K. K. (November 2014). Centrifugal Compressor Analysis by CFD. Mechanical Department, MITM, Indore, India.
8. Blazek, J. (2001). Computational Fluid Dynamics: Principles and Applications: Principles and Applications.
9. Bosman, B. V. (December 2012). Design of a Centrifugal Compressor Impeller for Micro Gas Turbine Application. MSc Thesis, Stellenbosch University, South Africa: Department of Mechanical and Mechatronic Engineering.
10. Bousquet, Y., Carbonneau, X., Dufour, G., Binder, N., and Trebinjac, I. (16 January 2014) Analysis of the Unsteady Flow Field in a Centrifugal Compressor from Peak Efficiency to Near Stall with Full-Annulus Simulations.
11. Braembussche, R. A. (March 2012). Micro Gas Turbines – A Short Survey of Design Problems. Von Karman Institute for Fluid Dynamic, Belgium.
12. Decuypere, R. and Verstraete, D. (2005). Micro Turbines from the Standpoint of Potential Users. Roya Military Academy of Belgium: Applied Fluid Mechanics Department.
13. De Villers, L. C. B. (December 2014). Design of a Centrifugal Compressor for Application in Micro Gas Turbines. MSc Thesis, Stellenbosch University, South Africa: Department of Mechanical and Mechatronic Engineering.

14. Flavio, C., Gabriele C, Leonardo P., and Sandro V. (September 2010). Micro Gas Turbines. Universita Politecnica delle Marche.
15. Habeeb, B. I. (2017). Design of a 1.2Kg Object Dropping UAV. Assessment for Aircraft Design (AAE 401). Kwara State University: Department of Aeronautical and Astronautical Engineering.
16. Hirano, T., Tsujita, H. Ronglei, G., and Gaku, M. (September 28, 2009). Design and Prototyping Micro Centrifugal Compressor for Ultra Micro Gas Turbine. Tokyo Metropolitan College of Industrial Technology: Production System Engineering Course.
17. Ismail, K. A. R., Rosolen, C. V. A. G., Benevenuto, F. J., and Lucato, D. (1998). Small Radial Compressors: Aerodynamic Design and Analysis. State University of Campinas, UNICAMP/FEM/DETF, C. P. 6112 Campinas, SP, Brasil CEP: 13083-970.
18. Jidai, W., Kunpeng L., Lan. M., Jihong, W., Mark, D., Shihong, M., Jian, L., and Dan, W. (13 July 2017). Overview of Compressed Air Energy Storage and Technology Development.
19. Kanpur, I. I. T. (12-16 April 2016). Introduction to Computational Fluid Dynamics; Computational Methods in Engineering Applications. Aligarh Muslim University, Aligarh: Department of Mechanical Engineering, Fluid Mechanics Group.
20. Krige, D. S. (March 2013). Performance Evaluation of a Micro Gas Turbine Centrifugal Compressor Diffuser. MSc Thesis, Stellenbosch University, South Africa. Department of Mechanical and Mechatronic Engineering.
21. Marcellan, A. (13 May 2015). An Exploration of Micro Turbines Based Propulsion Systems for Civil Unmanned Aerial Vehicles. MSc Thesis, Delft University of Technology: Aerospace Engineering.
22. Mayowa, A. E. (2018). Design and Optimization of a Centrifugal Compressor for a Micro Turbine Engine Powering a UAV.
23. Mayowa, A. (2017). Design and Optimization of a Mixed Flow Compressor Impeller for a Bladeless Fan. Ngwu Electronics, Enugu, Nigeria.
24. Meherwan, P. B. (2003). Centrifugal Compressors: A Basic Guide. Library of Congress Cataloging-in-Publication Data.

25. Mert C. (September 2009). Design and Optimization of a Mixed Flow Compressor Impeller Using Robust Design Methods. MSc Thesis, School of Natural and Applied Sciences, Middle East Technical University: Department of Aerospace Engineering.
26. Mohammad, H. S. (2013). Aircraft Design: A System Engineering Approach. Daniel Webster College, New Hampshire, USA.
27. Mohammed, M. K., Patra, S., and Lanzon, A. (August 2011). Designing Electric Propulsion System for UAVs. Control System Centre, EEE, University of Manchester, UK.
28. Pecnik, R., Rinaldi, E., and Colonna, P. (June 2012). Computational Fluid Dynamics of a Radial Compressor Operating with Supercritical CO_2. Delft University of Technology: Process and Energy Department.
29. Peer-Olaf, S. and Uwe, A. Introduction to Multi-Agent Simulation. School of Computer Science and IT (ASAP), University of Nottingham.
30. Prof. Nagpurwala, Q. H. Design of Centrifugal Compressor-1. M S Ramaiah School of Advanced Studies, Bengalure.
31. Prof. Nagpurwala, Q. H. Design of Centrifugal Compressor. M S Ramaiah School of Advanced Studies, Bengalure.
32. Shang, J. S. (October 2009). Computational Fluid Dynamics Application to Aerospace Science. Wright State University, Dayton, Ohio, USA.
33. Welliver, A. D., Acurie, I. (September 1967). Design and Development of Small, Single-Stage Centrifugal Compressor. U S. Army Aviation Materiel Laboratories. Fort Eustis, Virginia.
34. Xavier, M., Gianfranco, P., and Fernando, L. (November 17, 2014). Centrifugal Compressor Optimization. BSc Thesis, Florida International University: Department of Mechanical Engineering.